

A Design Strategy for Single-Molecule Magnet Materials with Fullerene Confinement-Induced Unpaired f-Electrons

Xiao-Kun Zhao,^{ab} Jing Zhao,^{ab} Shi-Ru Wei,^b Yun-Ze Qiu,^b Yang He,^b Han-Shi Hu^{*b} and Jun Li,^{*abc}

Affiliations

- a. Department of Chemistry and Guangdong Provincial Key Laboratory of Catalytic Chemistry, Southern University of Science and Technology, Shenzhen 518055, China.
- b. Department of Chemistry and Engineering Research Center of Advanced Rare-Earth Materials of Ministry of Education, Tsinghua University, Beijing 100084, China.
- c. Fundamental Science Center of Rare Earths, Ganjiang Innovation Academy, Chinese Academy of Sciences, Ganzhou 341000, China.

*Corresponding author email: hshu@mail.tsinghua.edu.cn (H.-S. H.); junli@tsinghua.edu.cn (J. L.)

Table of Contents

1. Computational details
2. Supplementary figures
3. Supplementary tables

1. Computational details

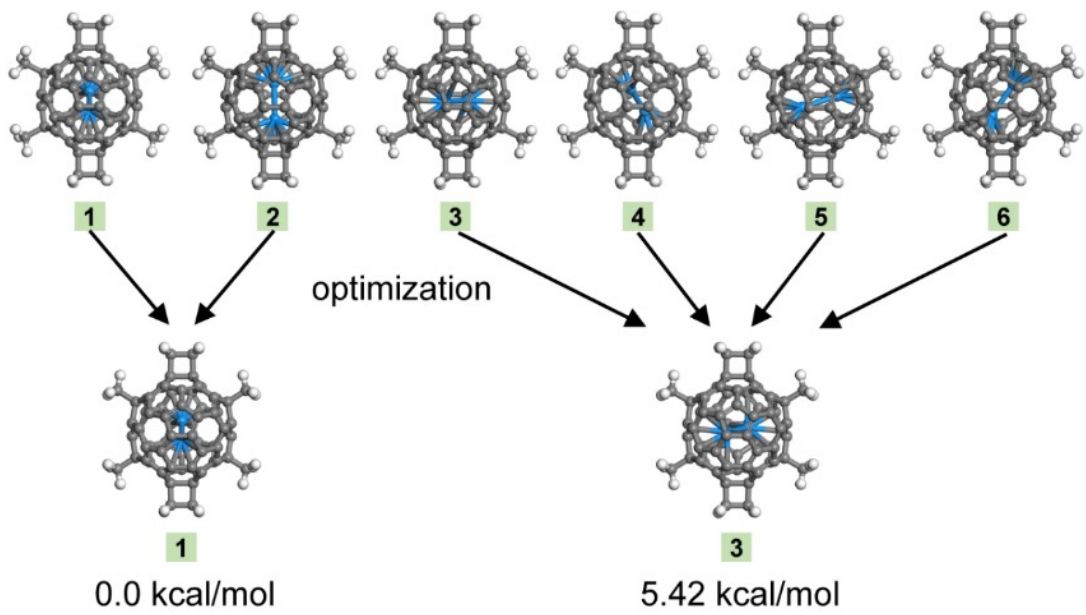
DFT parameters. Theoretical calculations were performed using the Kohn-Sham DFT on both supercell solids and cluster models. The supercell calculations were conducted with VASP 5.4.4, using the PBE exchange-correlation functional. A Plane-wave basis set with a 600 eV cutoff kinetic energy was applied to expand the valence electron densities. Core–valence interactions were handled with the projector-augmented wave (PAW) method.¹ To address correlation effects of 5f electrons, the Coulomb-corrected local spin-density approximation (LSDA + U) was employed with a Hubbard parameter ($U_{\text{eff}} = U - J$) of 4.0 eV for 5f electrons of uranium and 0 eV for thorium.² Band structure calculations for the 2D diactinide EMF

monolayers utilized the Heyd–Scuseria–Ernzerhof (HSE06) hybrid functional.³ Geometry optimization and self-consistent field convergence thresholds were set to 10^{-3} eV/Å and 10^{-6} eV, respectively. The Brillouin zone was sampled with a $2 \times 3 \times 1$ gamma-centered Monkhorst–Pack k-points grid, and van der Waals interactions were corrected using the DFT-D3 semi-empirical method.⁴

Stability analysis. Phonon dispersion analysis was carried out using the Phonopy code with the finite displacement method. For the crystal orbital Hamilton population (COHP) analysis, the LOBSTER 4.1.0 package was used to reconstruct orbital-resolved wavefunctions by projecting delocalized plane waves onto localized atomic-like basis sets.⁵ *Ab initio* molecular dynamics (AIMD) simulations were carried out using the Quickstep module with the PBE functional, implemented in the CP2K package.⁶ Mixed Gaussian and plane-wave basis sets, with a plane-wave cutoff of 500 Ry, were applied.⁷ Molecularly optimized double- ζ valence plus polarization basis sets were used. Geodecker–Teter–Hutter (GTH) pseudopotentials developed by Lu et al. were used for core electrons, with valence electrons of 14 for U, 12 for Th, and 4 for C.⁸ Initial configurations of 2D diactinide EMFs monolayers, using a 2×2 supercell (240 C atoms, 8 Th or U atoms) were annealed during AIMD simulations. Each AIMD simulation, conducted in the canonical (NVT) ensemble, had a time step of 1 fs, with temperature control using Nose–Hoover thermostats.^{9,10}

Cluster models. $U_2@C_{60}$, $Th_2@C_{60}$, $U_2@C_{66}H_{20}$, and $Th_2@C_{66}H_{20}$ cluster models were calculated using AMS2023 software.¹¹ Scalar relativistic effects were considered with the zero-order regular approximation (ZORA),¹² and Slater-type-orbital (STO) basis sets of triple- ζ plus polarization functions (TZP) quality were used with the BP86 and PBE0 functionals.^{13,14} Complete active space self-consistent field (CASSCF) calculations were performed using ORCA 5.0 software¹⁵ with SARC-DKH-TZVP basis set for U and Th,¹⁶ and def2-SV(p) basis set for C and H.¹⁷ Energy decomposition analysis with natural orbitals for chemical valence (EDA-NOCV)¹⁸ was performed for cluster dimer models $(C_{66}H_{20})_2$, $(U_2@C_{66}H_{20})_2$, and $(Th_2@C_{66}H_{20})_2$. Principal Interacting Orbital (PIO) analysis¹⁹ of the $U_2@C_{60}$ model was performed using Gaussian 16 software,²⁰ with Stuttgart energy-consistent relativistic pseudopotential (ECP78MWB) and the corresponding ECP78MWB-AVTZ basis set²¹ for U and Th, and def2-SVP basis set for C and H.

2. Supplementary Figures



Figs. S1. The most favorable position of the encapsulated U_2 dimer in the optimized $\text{U}_2@\text{C}_{66}\text{H}_{20}$ cluster model.

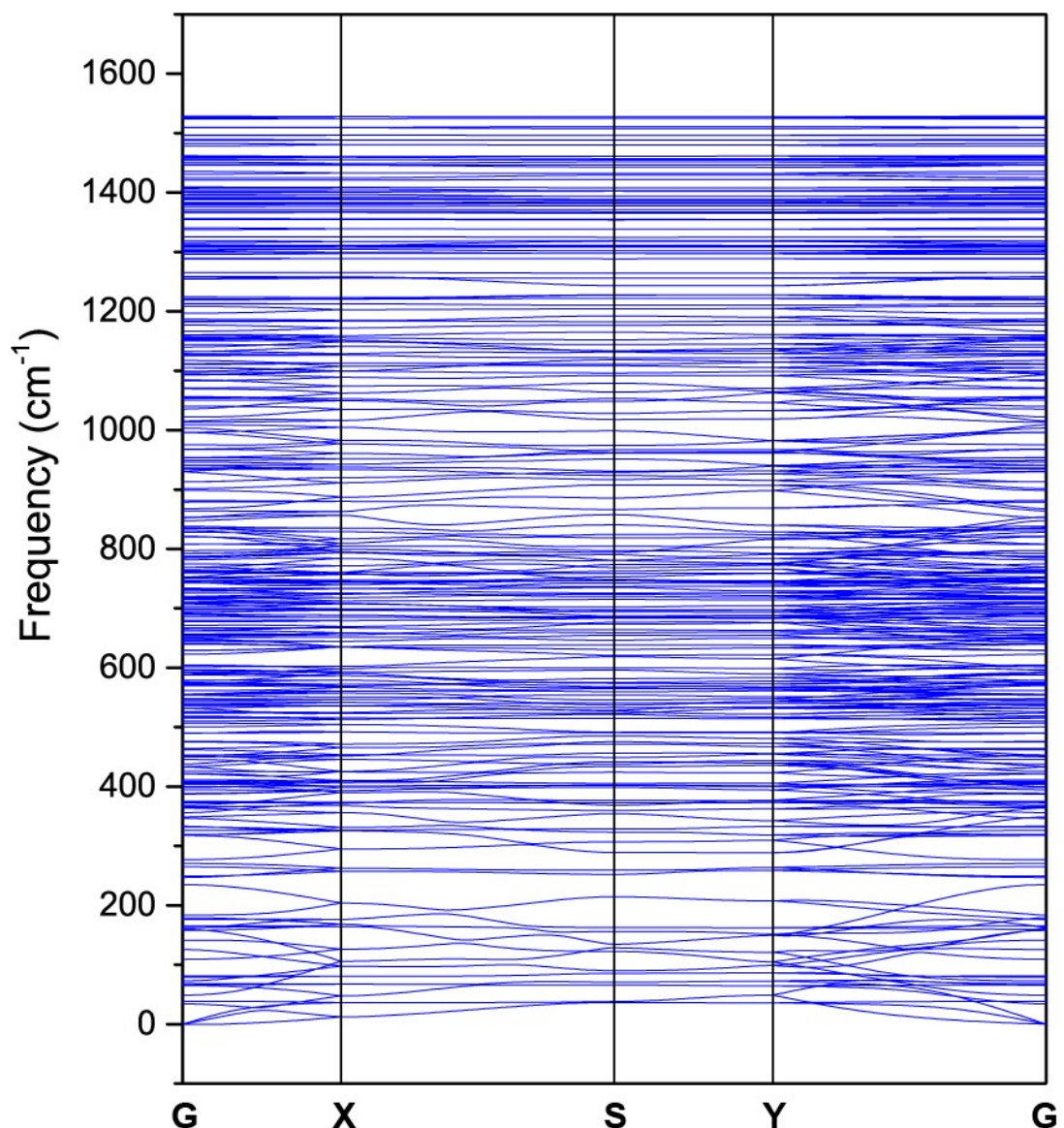


Fig. S2. The phonon spectrum of $\text{U}_2@\text{C}_{60}$ -2D monolayer.

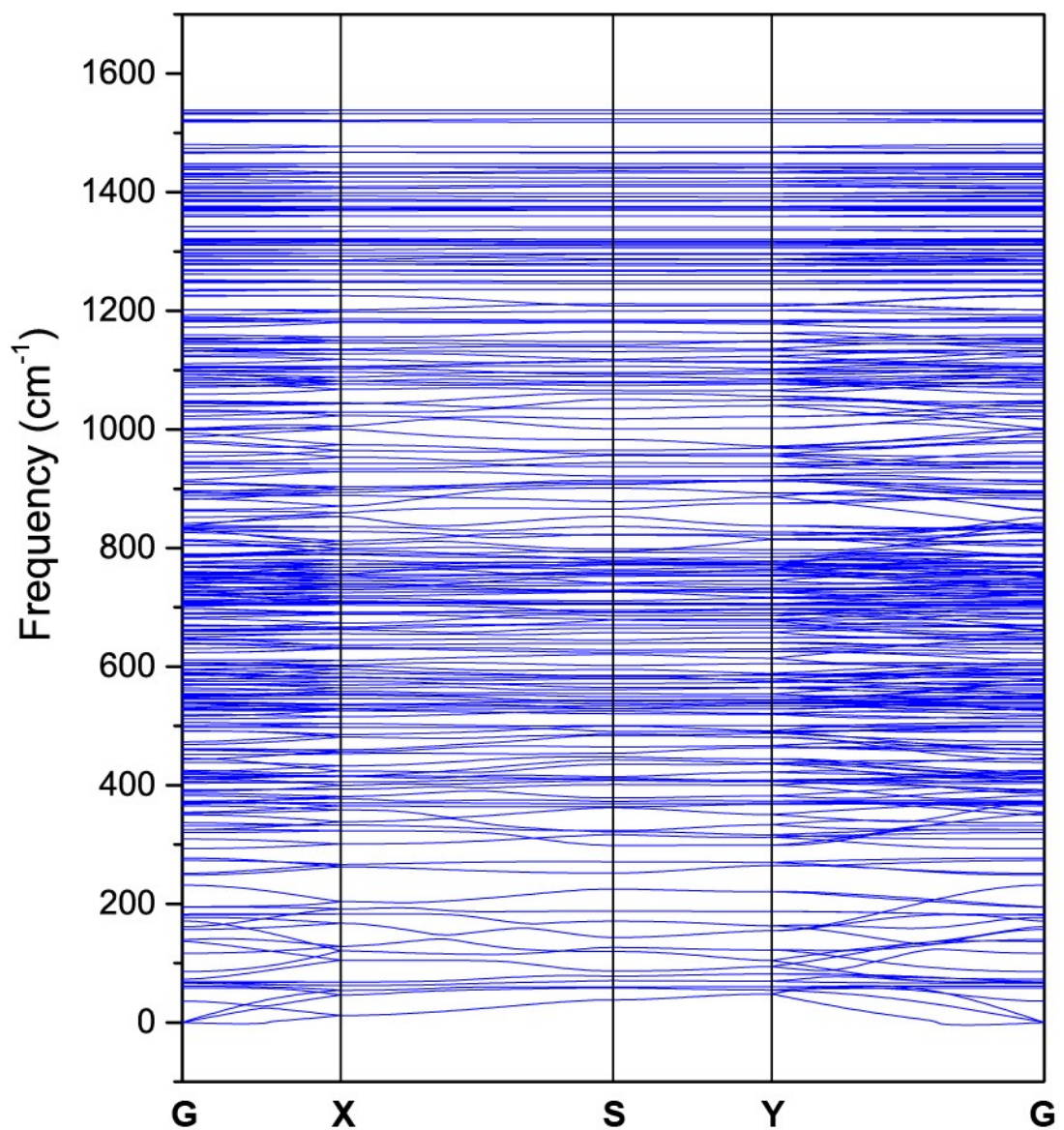


Fig. S3. The phonon spectrum of $\text{Th}_2@\text{C}_{60}$ -2D monolayer.

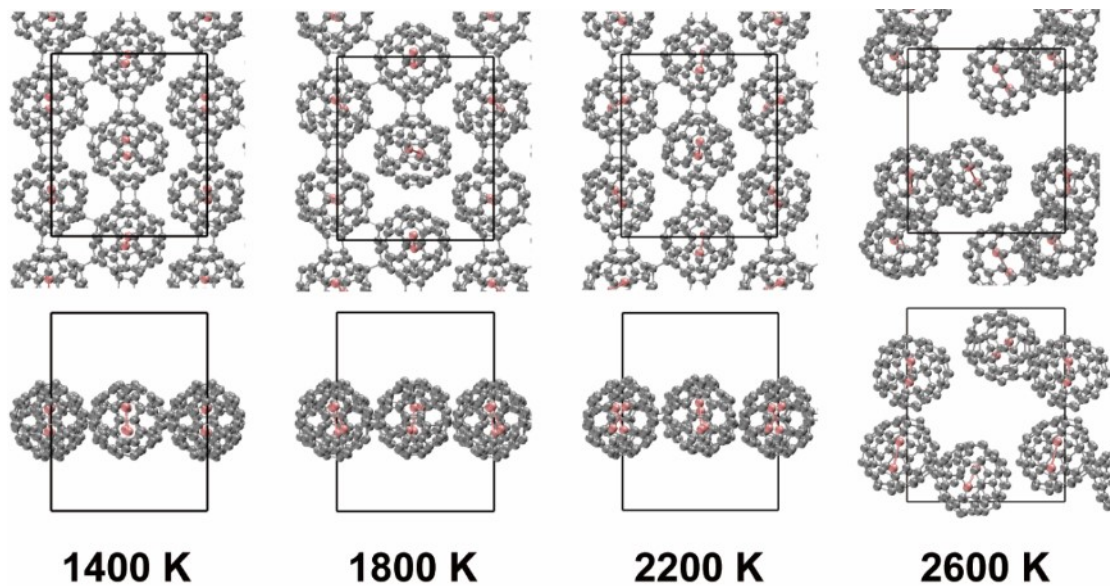


Fig. S4. The snapshots of the final frame of each 10-ps AIMD simulations of $\text{U}_2@\text{C}_{60}$ -2D monolayer from 1400 K to 2600 K (top and side views).

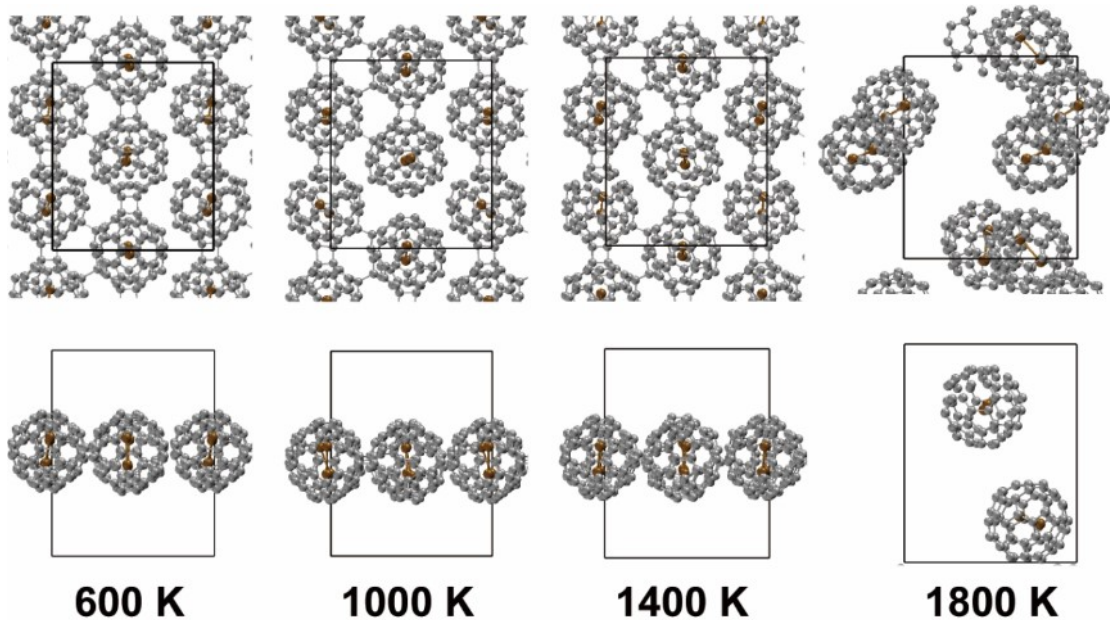


Fig. S5. The snapshots of the final frame of each 10-ps AIMD simulations of $\text{Th}_2@\text{C}_{60}$ -2D monolayer from 600 K to 1800 K (top and side views).

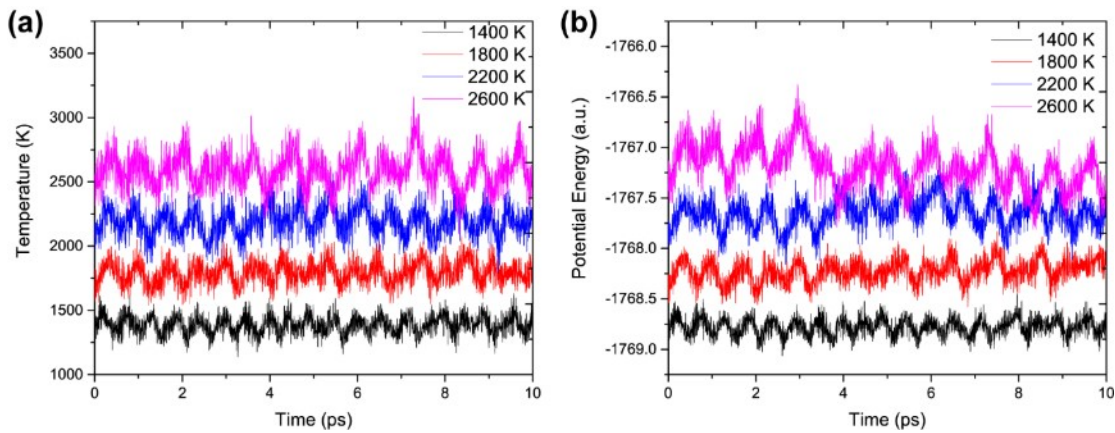


Fig. S6. Fluctuations of (a) temperature and (b) total potential energy for the $\text{U}_2@\text{C}_{60}$ -2D monolayer at different temperatures during the AIMD simulations.

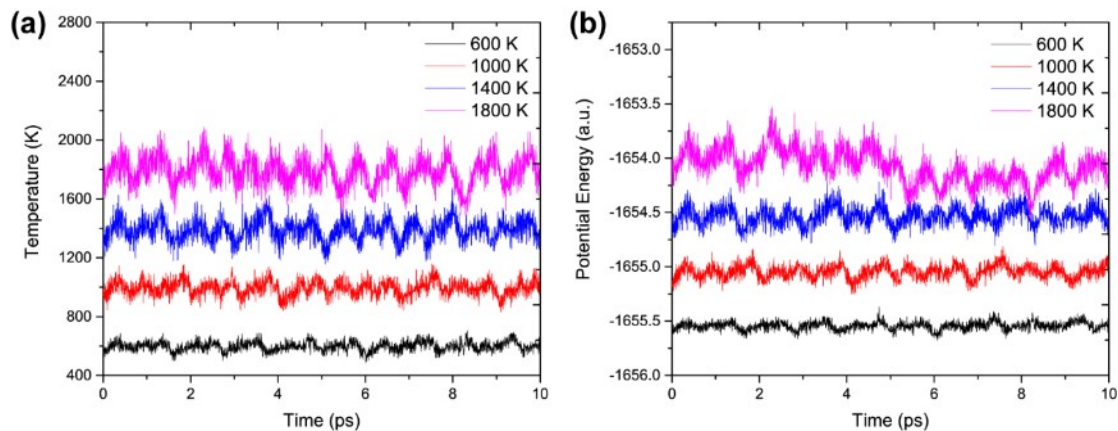


Fig. S7. Fluctuations of (a) temperature and (b) total potential energy for the $\text{Th}_2@\text{C}_{60}$ -2D monolayer at different temperatures during the AIMD simulations.

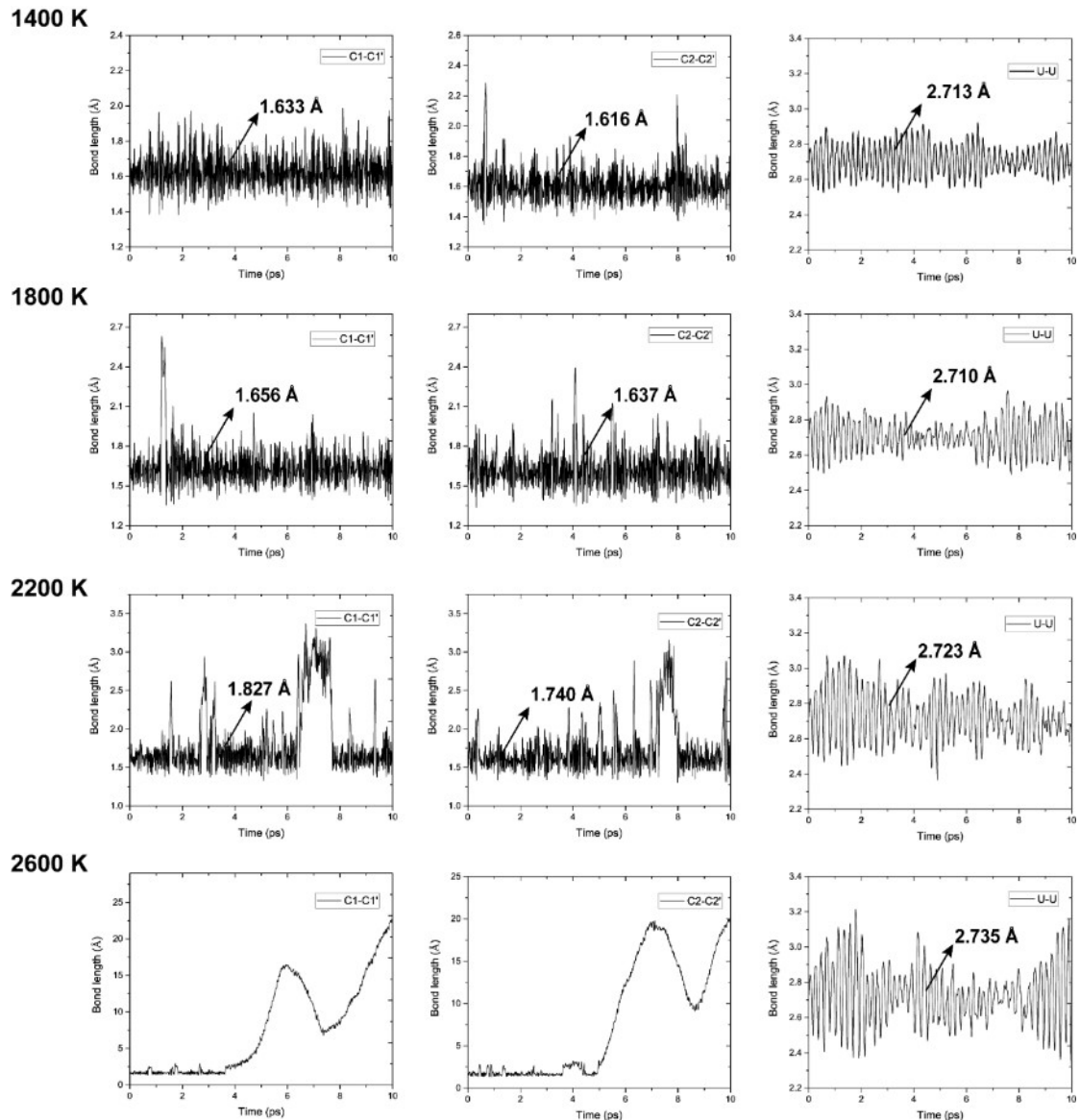


Fig. S8. The changes of bond lengths of C1-C1' and C2-C2' in U₂@C₆₀-2D monolayer at different temperatures (from 1400 K to 2600 K) during the AIMD simulations. The value indicated by the arrow represents the average bond length during the simulations.

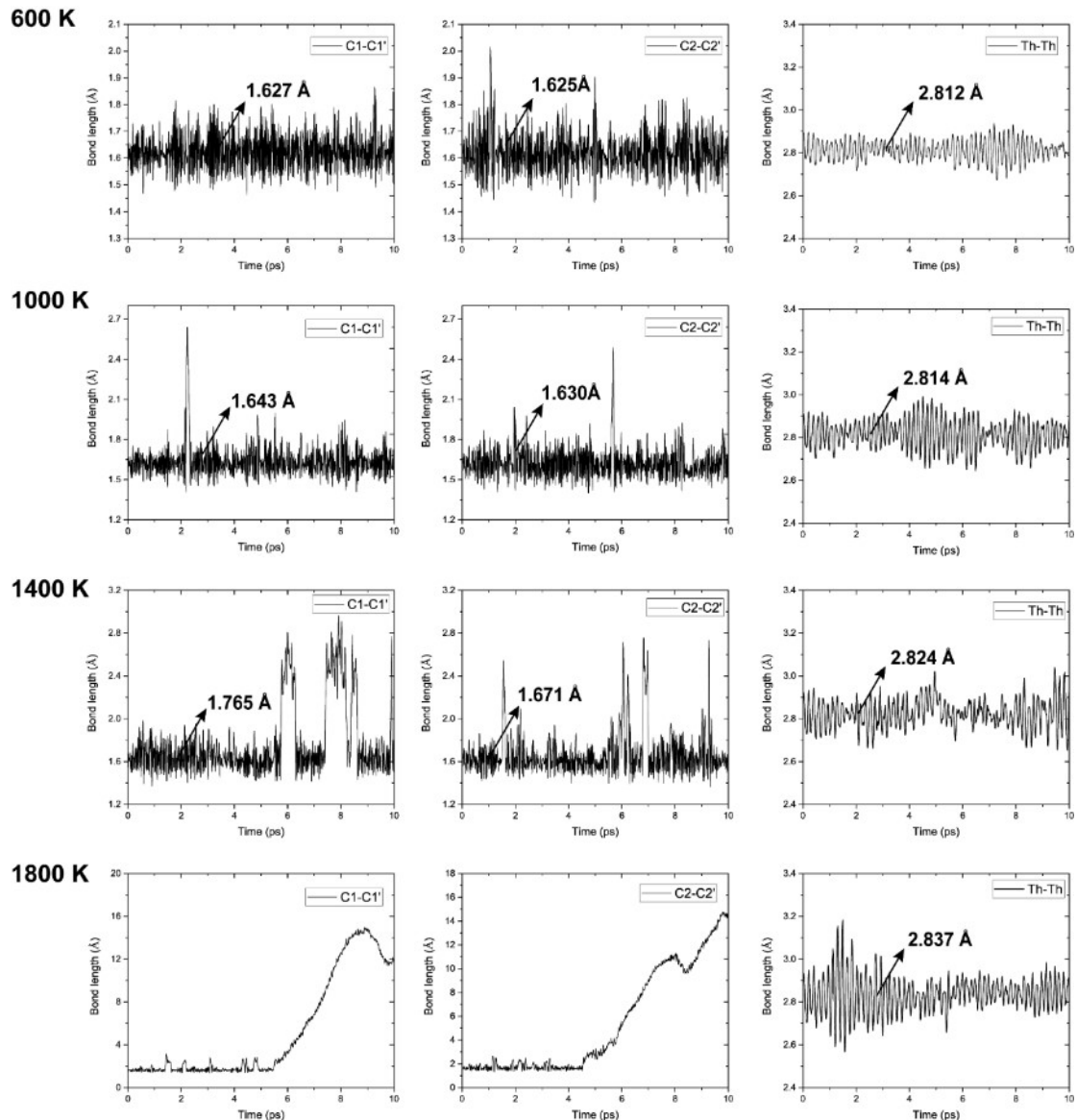


Fig. S9. The changes of bond lengths of $\text{C}1-\text{C}1'$ and $\text{C}2-\text{C}2'$ in $\text{Th}_2@\text{C}_{60}$ -2D monolayer at different temperatures (from 600 K to 1800 K) during the AIMD simulations. The value indicated by the arrow represents the average bond length during the simulations.

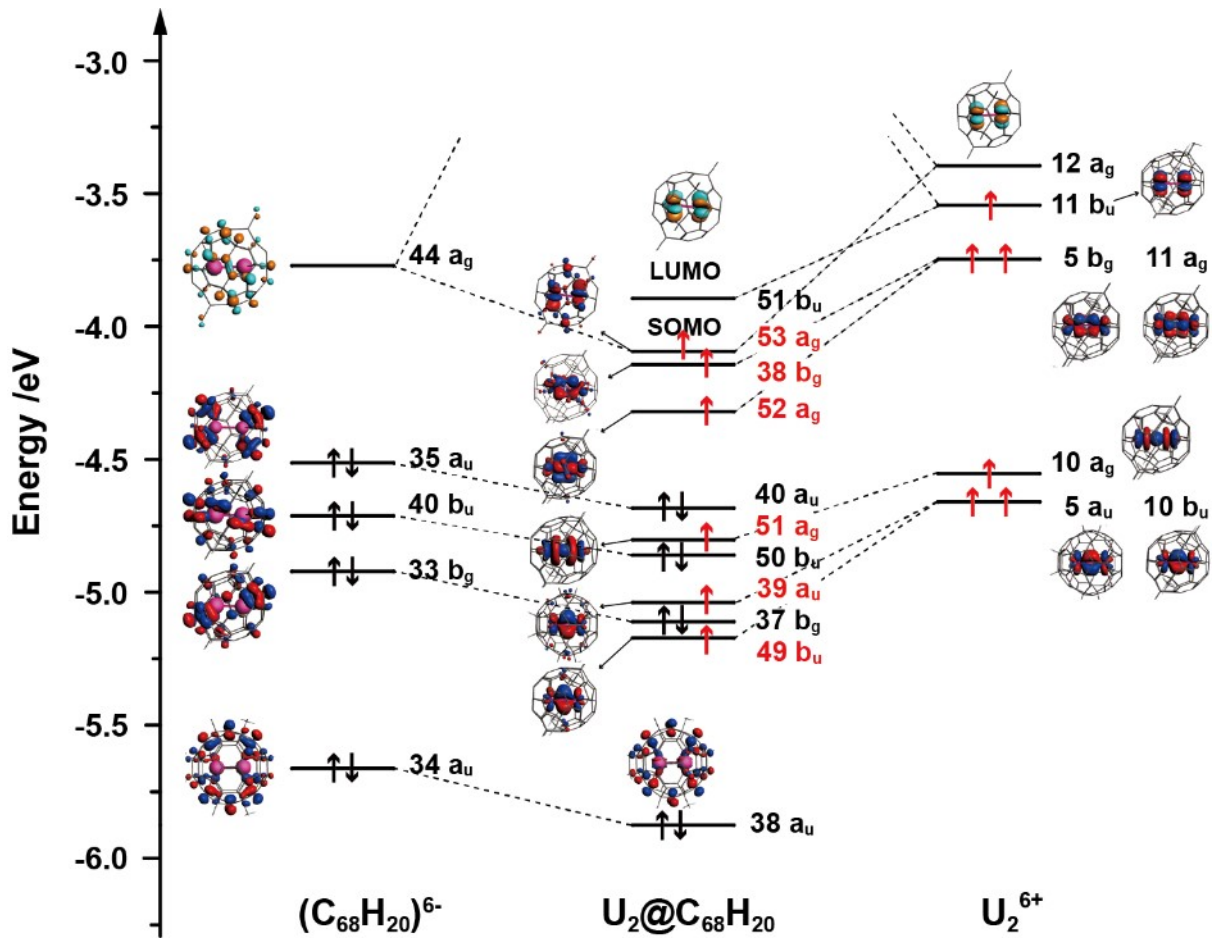


Fig. S10. Orbital interaction diagram for $\text{U}_2@\text{C}_{68}\text{H}_{20}$ molecular model illustrating the bonding scheme between $(\text{C}_{68}\text{H}_{20})^{6-}$ and U_2^{6+} fragment ($\text{iso} = 0.04$). The red arrows represent the unpaired electrons from the U_2^{6+} fragment, and the black arrows represent the electrons from the $(\text{C}_{68}\text{H}_{20})^{6-}$ fragment. ($\text{isovalue} = 0.03$ a.u.)

The triply degenerate LUMO (t_{1u}) of neutral C_{60} (I_h) splits into the 33 b_g , 40 b_u , and 35 a_u frontier molecular orbitals (MOs) in the $\text{C}_{68}\text{H}_{20}$ (C_{2h}) molecule. As shown in **Fig. S10**, in the $\text{U}_2@\text{C}_{68}\text{H}_{20}$ molecule, these MOs are occupied by six electrons transferred from the encapsulated U_2 dimer. Although the bare $(\text{U}_2)^{6+}$ fragment has a $(5f\sigma_g)^1(5f\pi_u)^2(5f\delta_g)^2(5f\varphi_u)^1$ electronic structure with six single-electron bonds ($5a_u$, $10b_u$, $10a_g$, $5b_g$, $11a_g$, and $11b_u$), the unoccupied $12a_g$ orbital of the encapsulated $(\text{U}_2)^{6+}$ fragment can interact with the $44a_g$ orbital of the $\text{C}_{68}\text{H}_{20}$ molecule, leading to a non-bonding SOMO ($53a_g$). Consequently, there are five single-electron U–U bonds with $(5f\sigma_g)^1(5f\pi_u)^2(5f\delta_g)^2(5f\varphi_g)^1$ electronic structure in $\text{U}_2@\text{C}_{68}\text{H}_{20}$ molecule.

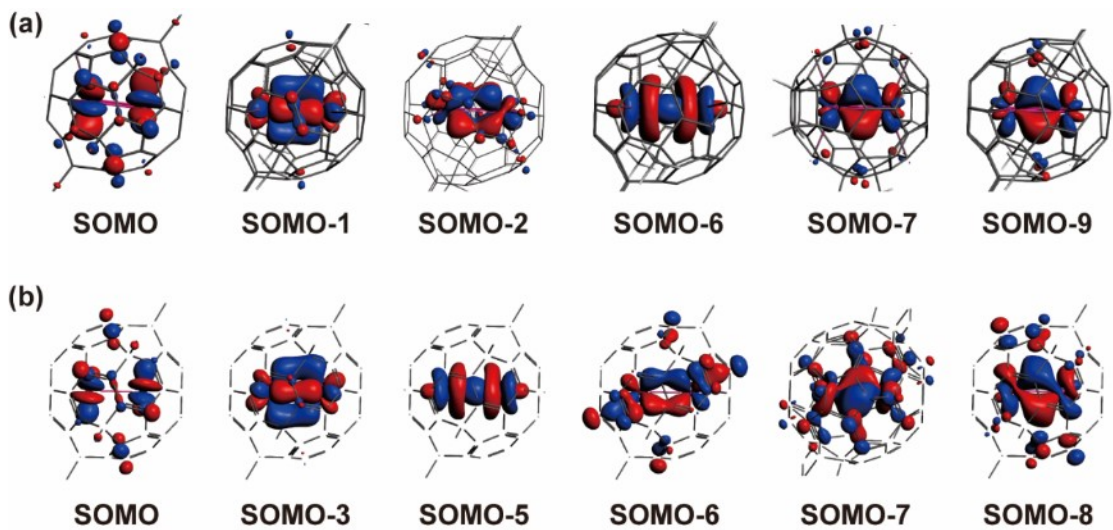


Fig. S11. The Kohn-Sham orbitals of U_2 dimer in $\text{U}_2@\text{C}_{68}\text{H}_{20}$ molecular model at (a) BP86/TZP and (b) PBE0/TZP level. (isovalue = 0.03 a.u.)

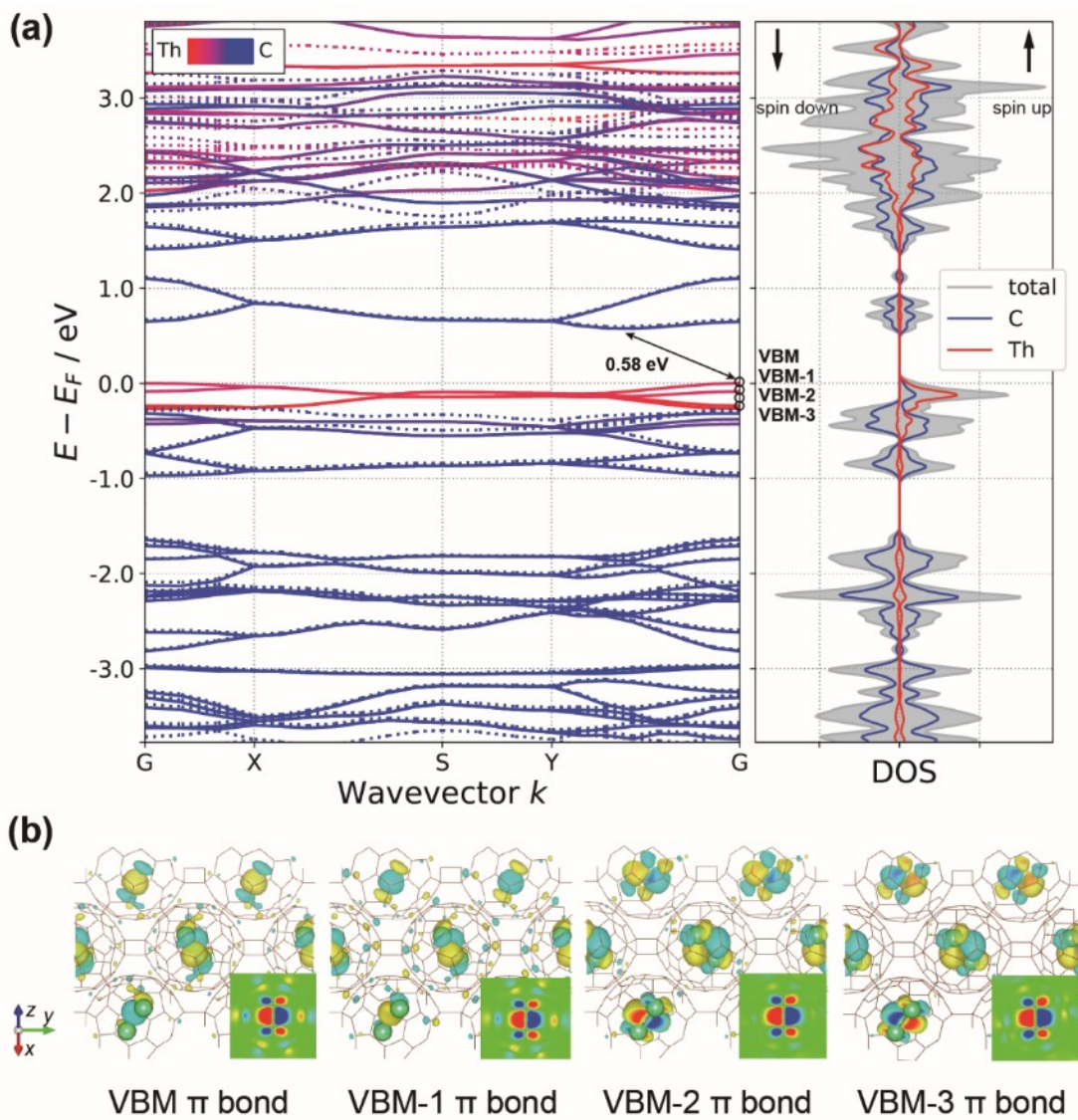


Fig. S12. (a) The Band structure and projected density of states (pDOS) at HSE06 level for $\text{Th}_2@\text{C}_{60}$ -2D monolayer. The four points of G (0, 0, 0), X (0.5, 0, 0), S (0.5, 0.5, 0) and Y (0, 0.5, 0) refer to the high-symmetry points of the first Brillouin zone in reciprocal space. The red curves are contributed by Th, and the blue curves are contributed by C. The solid lines and dash lines represent spin-up and spin-down bands, respectively. (b) The spin-up real space wavefunctions for bands at the gamma point represent the bonding patterns of the Th_2 dimer in the $\text{Th}_2@\text{C}_{60}$ -2D monolayer. The 2D contour plots in the lower left corner were sliced along the Th_2 dimer plane to provide a clear understanding of the bonding patterns of the Th_2 dimer. Note that the calculated model contains two EMF cages, thus there are two Th–Th π bonds in each fullerene.

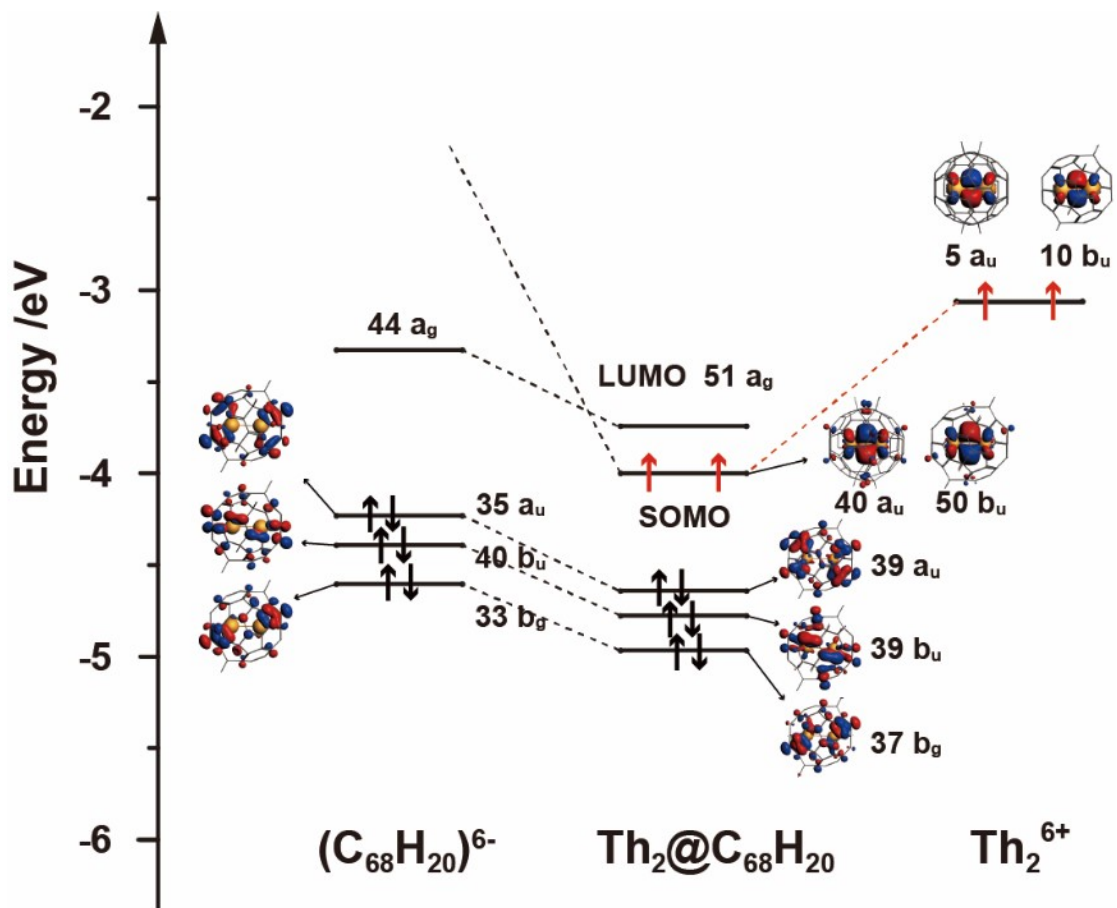


Fig. S13. Orbital interaction diagram for $\text{Th}_2@\text{C}_{68}\text{H}_{20}$ molecular model illustrating the bonding scheme between $(\text{C}_{68}\text{H}_{20})^{6-}$ and Th_2^{6+} fragment ($\text{iso} = 0.04$). The red arrows represent the unpaired electrons from the Th_2^{6+} fragment, and the black arrows represent the electrons from the $(\text{C}_{68}\text{H}_{20})^{6-}$ fragment. ($\text{isovalue} = 0.03 \text{ a.u.}$)

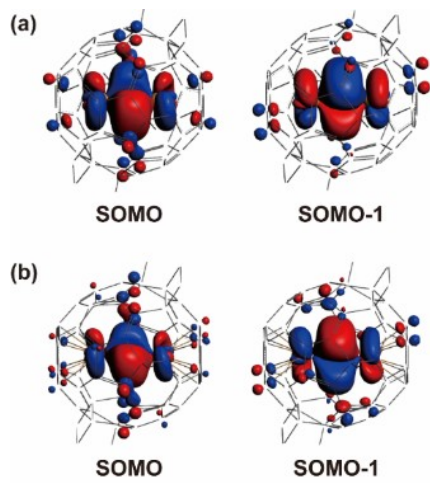


Fig. S14. The Kohn-Sham orbitals of Th_2 dimer in $\text{Th}_2@\text{C}_{68}\text{H}_{20}$ molecular model at (a) BP86/TZP and (b) PBE0/TZP level. (isovalue = 0.03 a.u.)

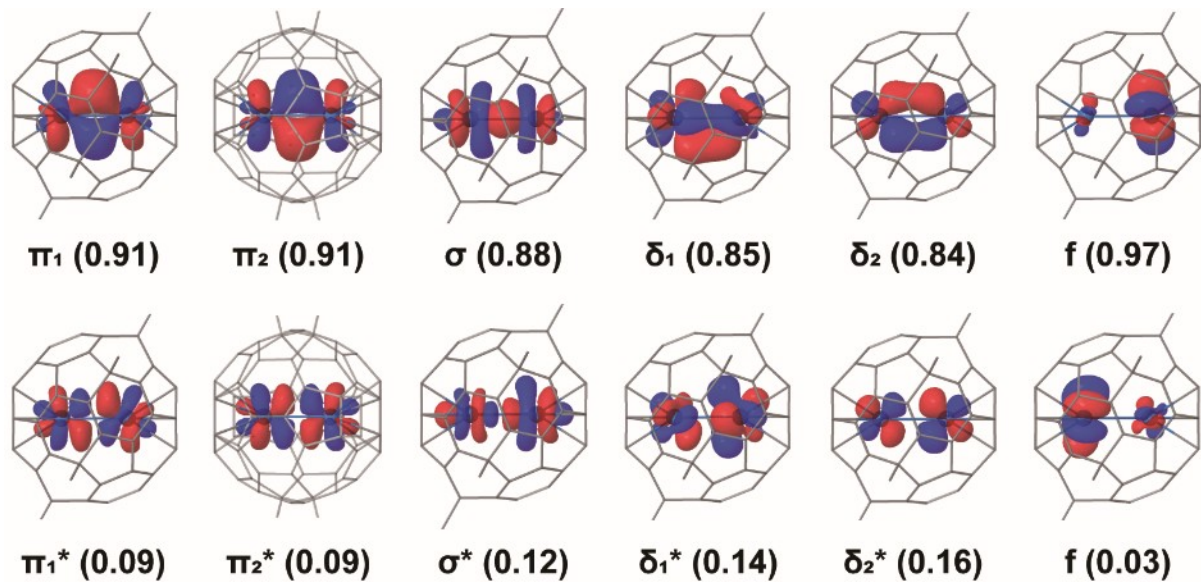


Fig. S15. Natural valence orbitals of U_2 dimer in $\text{U}_2@\text{C}_{68}\text{H}_{20}$ molecular model from CASSCF(6e, 12o) calculation. Orbital electron populations are in parentheses. The hydrogen atoms are omitted for clarity. Effective bond order = 1.90. (isovalue = 0.03 a.u.)

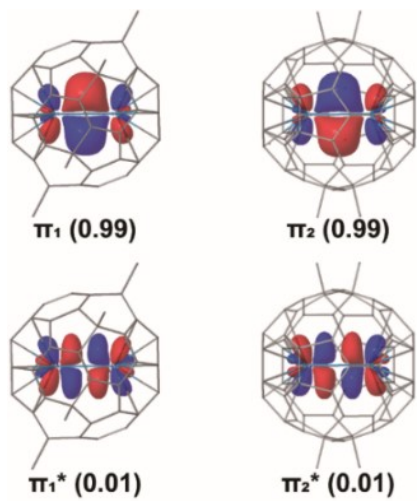


Fig. S16. Natural valence orbitals of Th_2 dimer in $\text{Th}_2@\text{C}_{68}\text{H}_{20}$ molecular model from CASSCF(2e, 4o) calculation. Orbital electron populations are in parentheses. The hydrogen atoms are omitted for clarity. Effective bond order = 0.98. (isovalue = 0.03 a.u.)

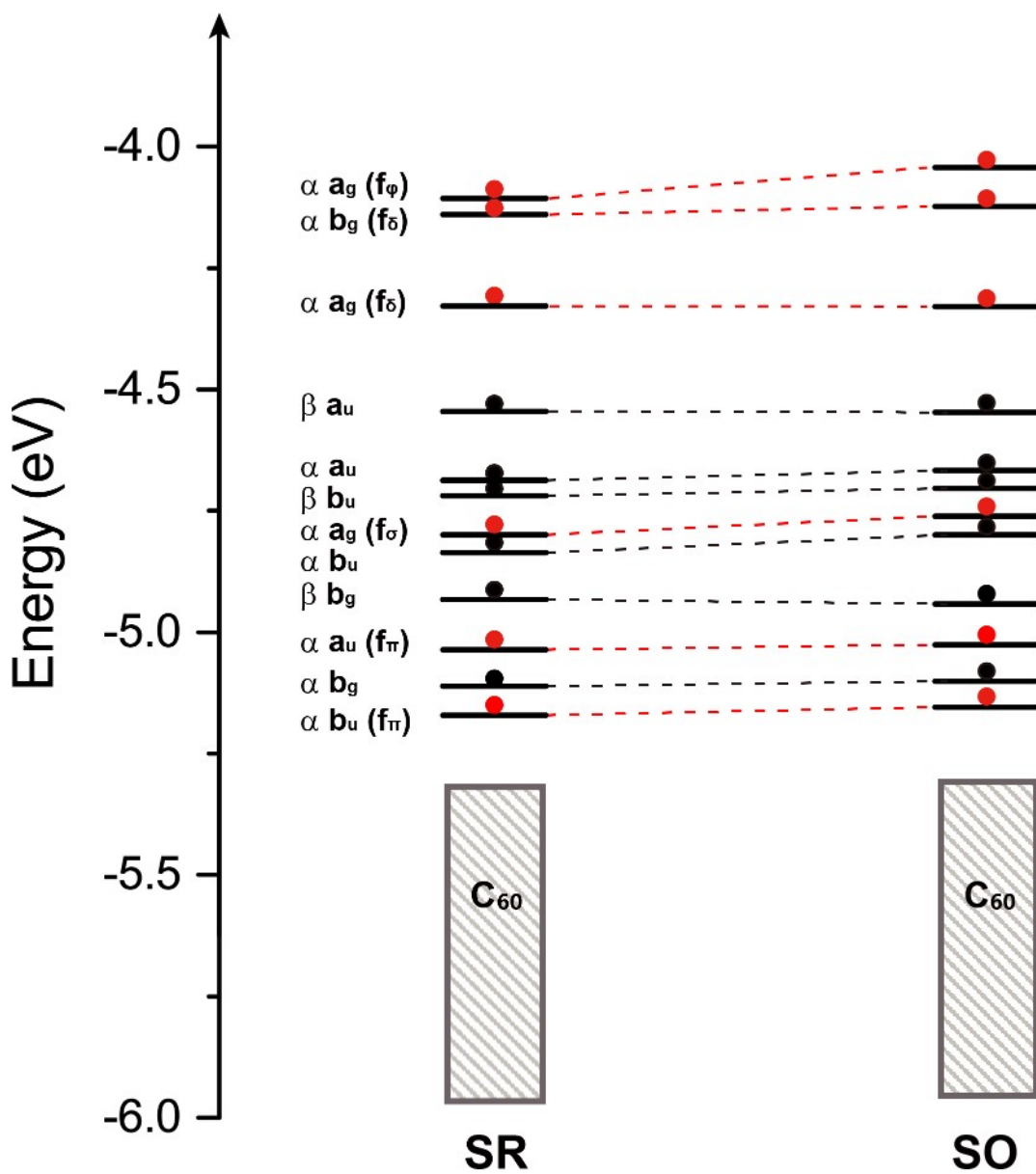


Fig. S17. Unrestricted Scalar relativistic (SR) and spin-orbit (SO) coupling relativistic molecular orbital (MO) energy levels of $\text{U}_2@\text{C}_{60}\text{H}_{20}$ molecular model, with the electrons on U orbitals and C orbitals marked by red and black dots, respectively. The black shadows represent the MOs from the fullerene cage.

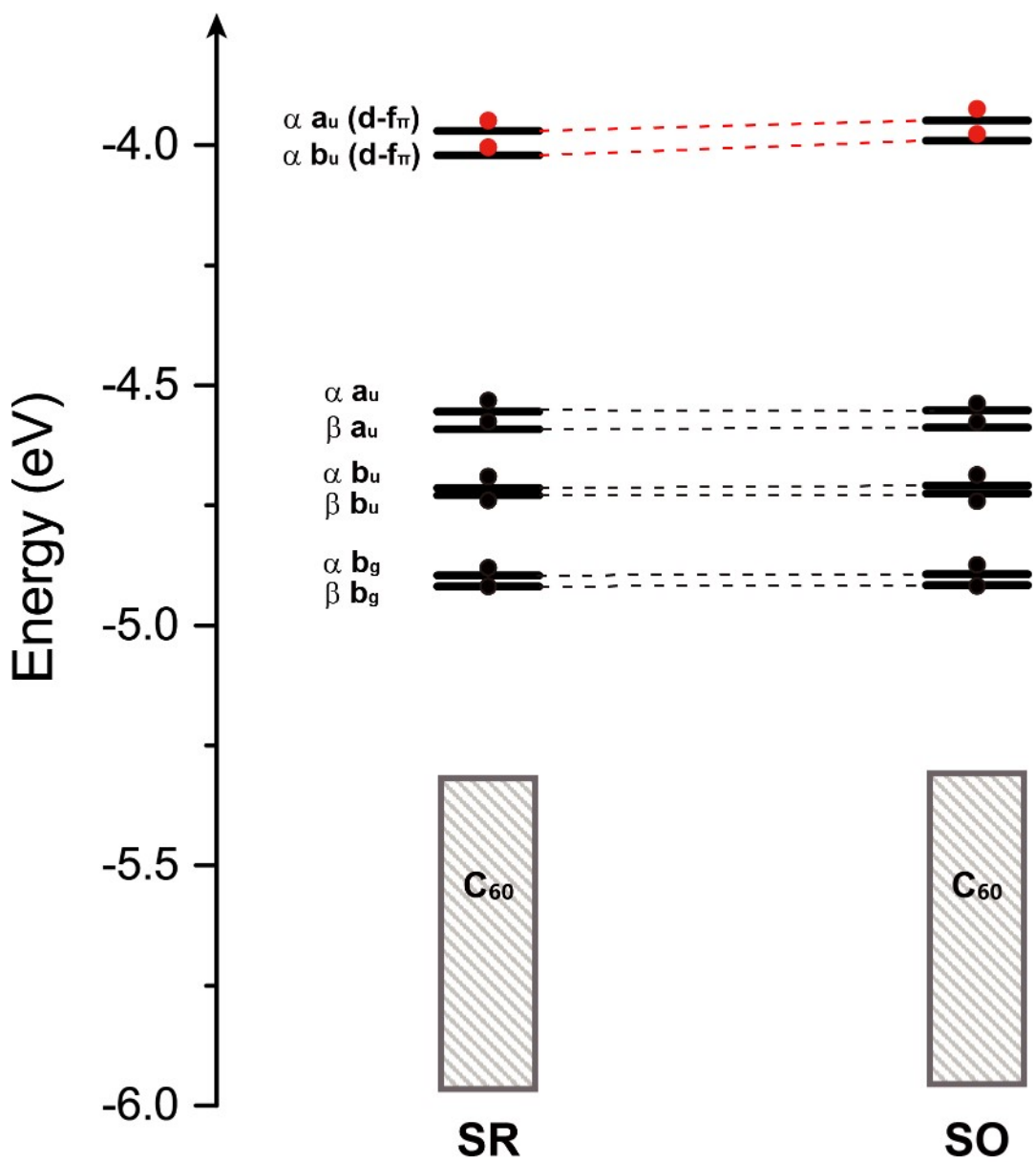


Fig. S18. Unrestricted Scalar relativistic (SR) and spin-orbit (SO) coupling relativistic molecular orbital (MO) energy levels of $\text{Th}_2@\text{C}_{60}\text{H}_{20}$ molecular model, with the electrons on Th orbitals and C orbitals marked by red and black dots, respectively. The black shadows represent the MOs from the fullerene cage.

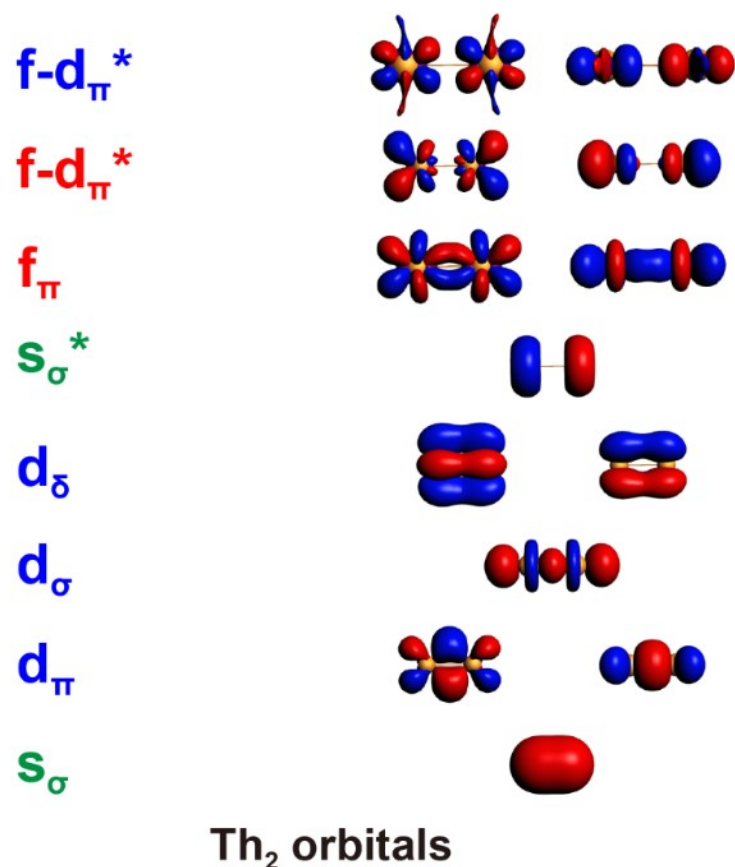


Fig. S19. The Kohn-Sham orbitals of the neutral Th₂ dimer. (isovalue = 0.03 a.u.)

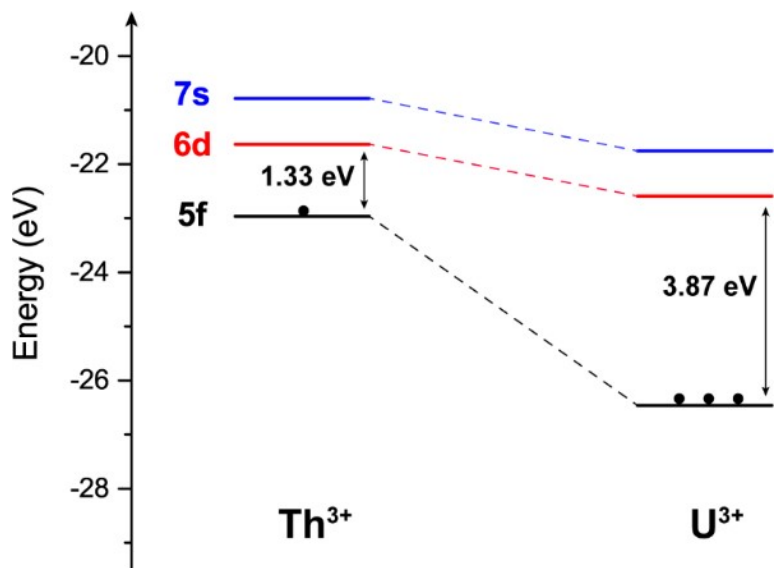


Fig. S20. Energy levels of the 7s, 6d, and 5f orbitals in Th³⁺ and U³⁺ ions.

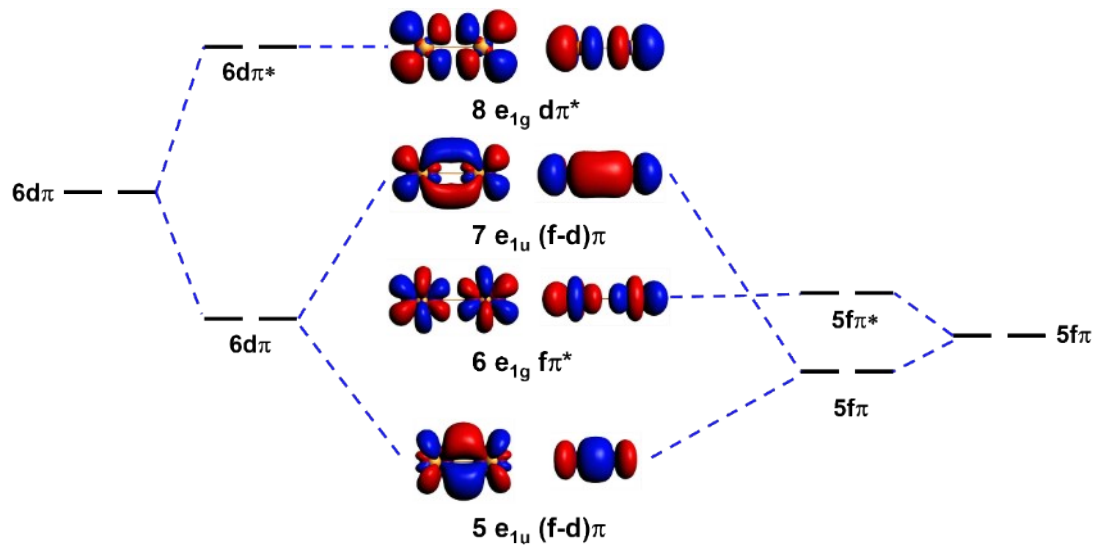


Fig. S21. The hybridization of the 6d and 5f orbitals in the Th₂⁶⁺ dimer result in the formation of two stable (f-d) π bonding orbitals, two less stable (f-d) π bonding orbitals, two f π^* antibonding orbitals, and two d π^* antibonding orbitals. (isovalue = 0.03 a.u.)

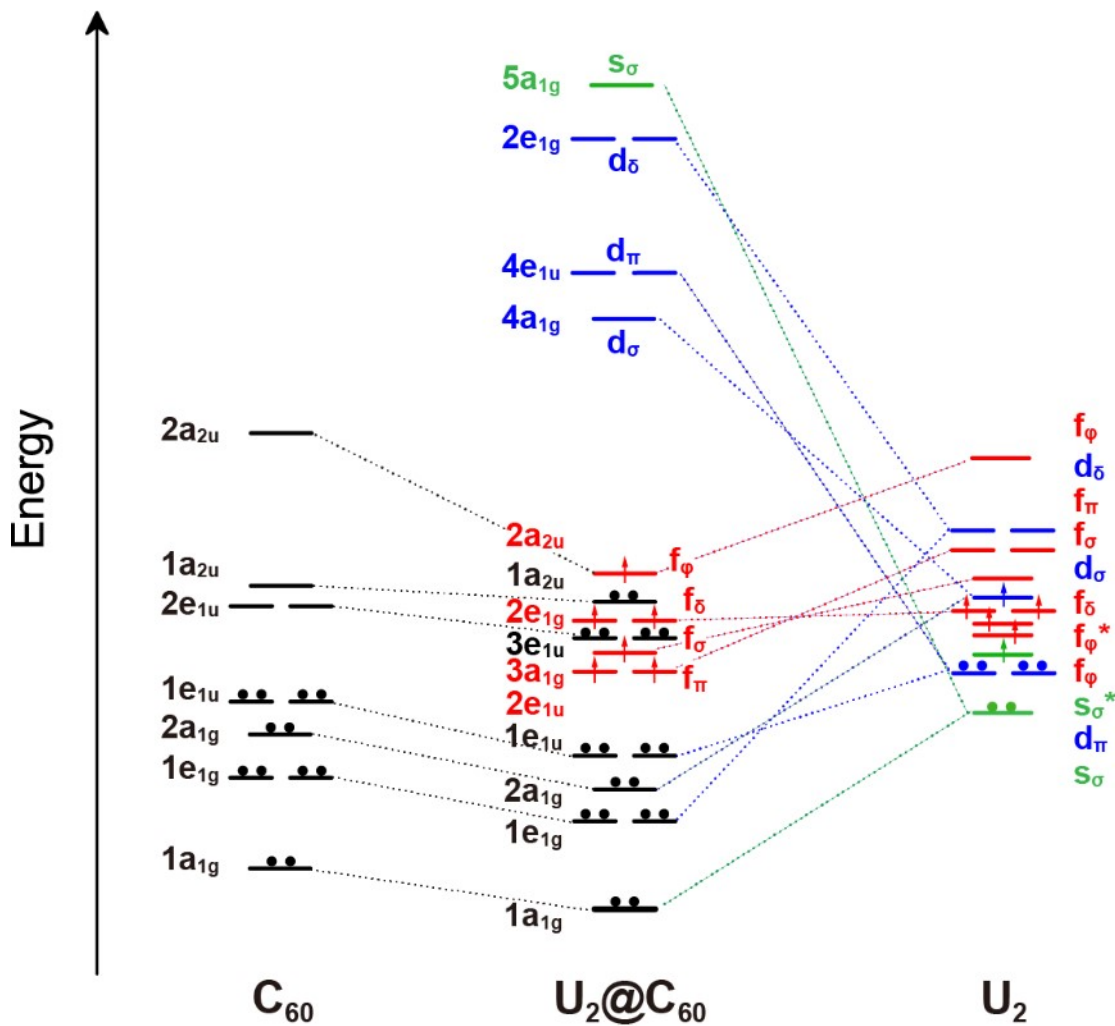


Fig. S22. Orbital interaction diagram for $\text{U}_2@\text{C}_{60}$ molecules, illustrating the bonding scheme between neutral C_{60} and U_2 dimer. The arrows represent the unpaired single-electron bonds of U_2 dimer, and the dots represent the electron-pair bonds.

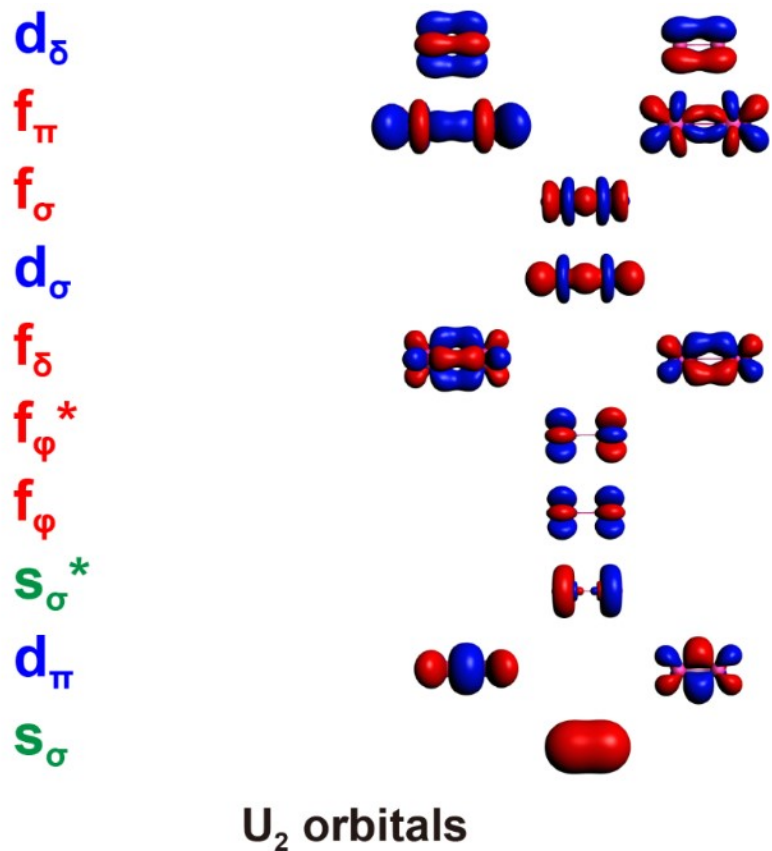


Fig. S23. The Kohn-Sham orbitals of the neutral U₂ dimer. (isovalue = 0.03 a.u.)

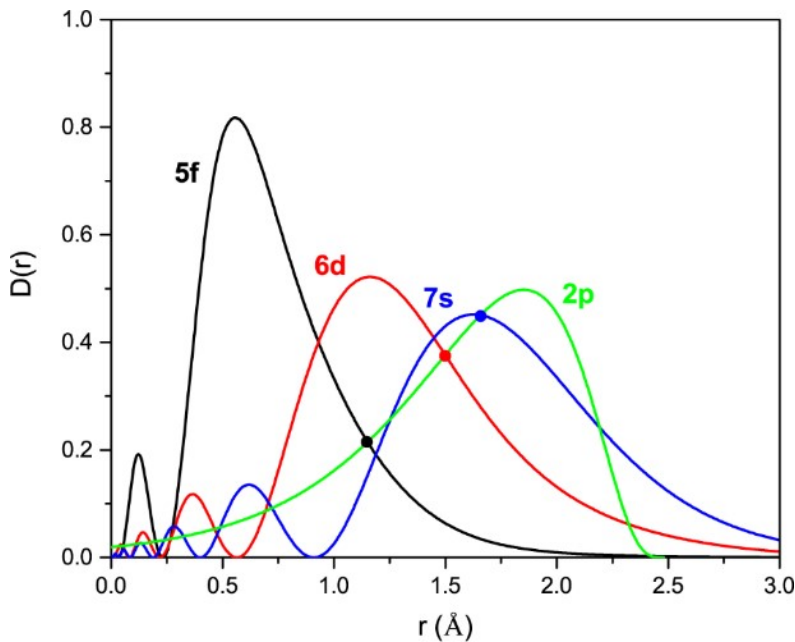


Fig. S24. Atomic valence-orbital radial distribution functions $D(r) = r^2R(r)^2$ for the 5f (black line), 6d (red line), and 7s (blue line) orbitals of U atom, and the 2p orbitals (green line) of the C atom, with a U–C bond length of 2.482 Å.

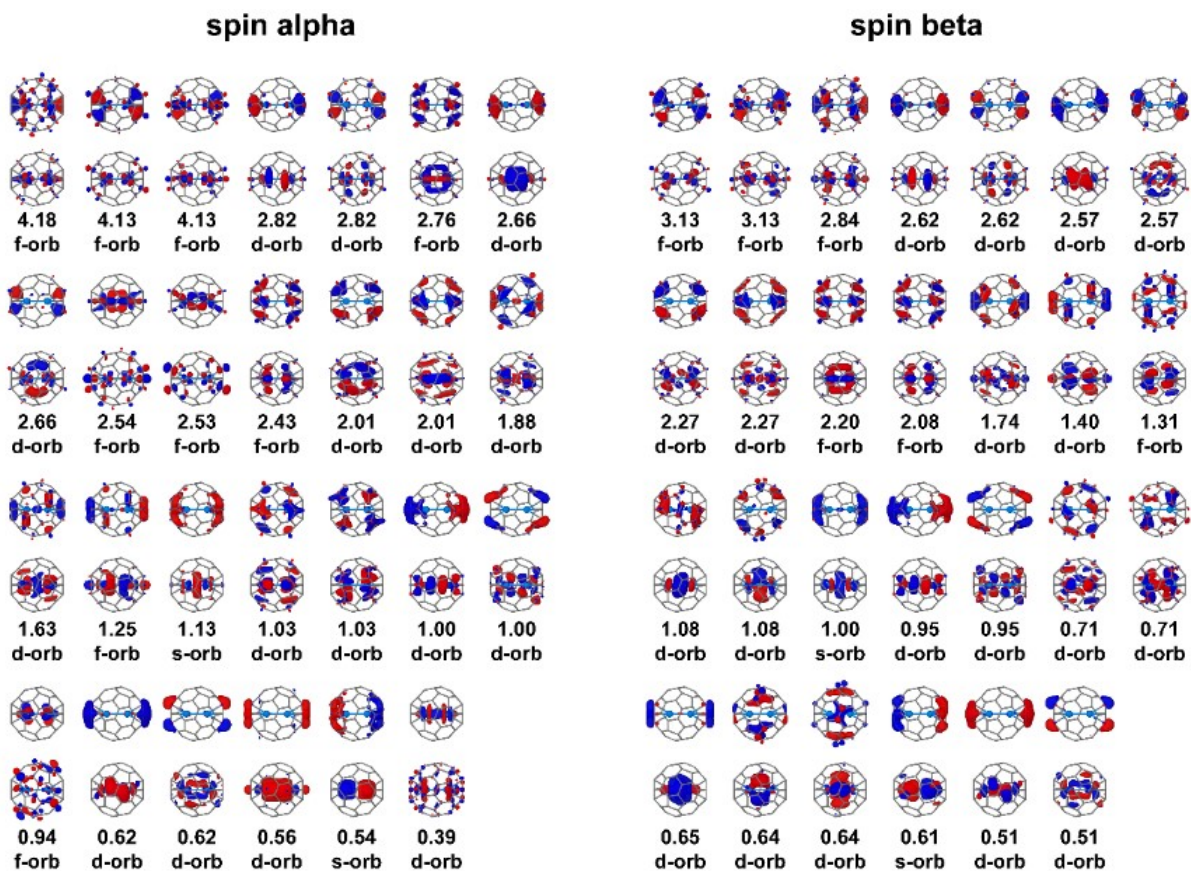


Fig. S25. In-phase (top) and out-of-phase (bottom) combinations of Principal Interacting Molecular Orbitals (PIMOs) between the U_2 and C_{60} fragments. The PIMOs listed account for 94.1% of the total interactions, with d orbitals contributing 52.5% and f orbitals contributing 38.2%. These values represent a percentage of each orbital's contribution to the interaction. (isovalue = 0.03 a.u.)

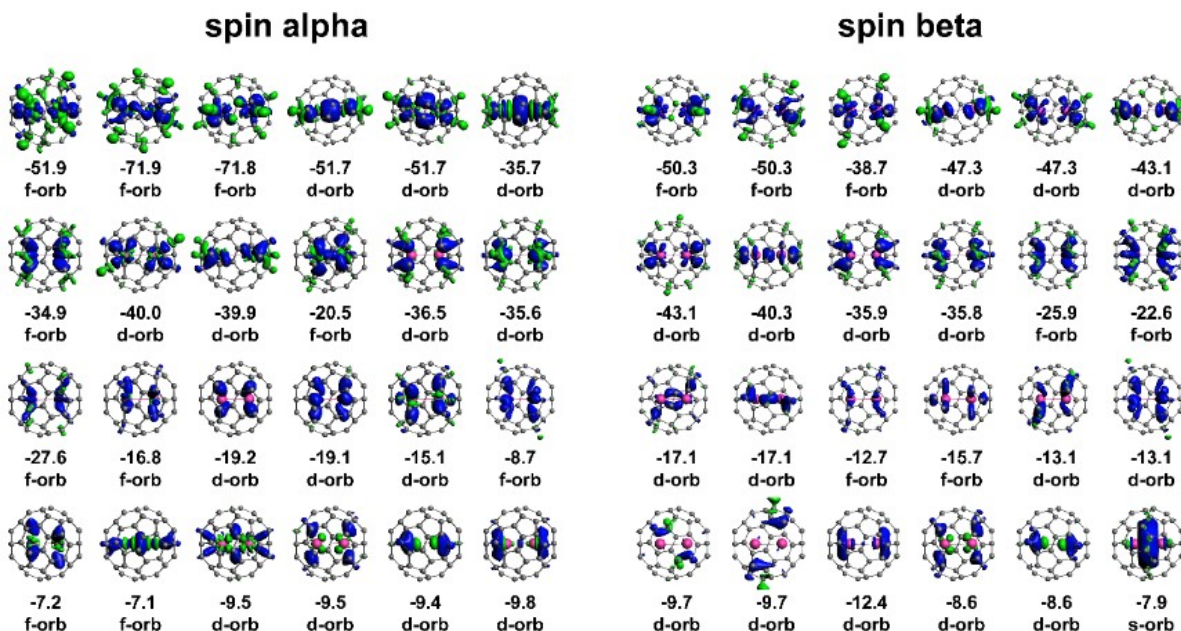


Fig. S26. NOCV density pairs between the U_2^{6+} and $(\text{C}_{60})^{6-}$ fragments. The listed NOCV density pairs account for 84.6% of the total interactions, with d orbitals contributing 50.0% and f orbitals contributing 34.1%. Energy values are given in $\text{kcal}\cdot\text{mol}^{-1}$. (isovalue = 0.03 a.u.)

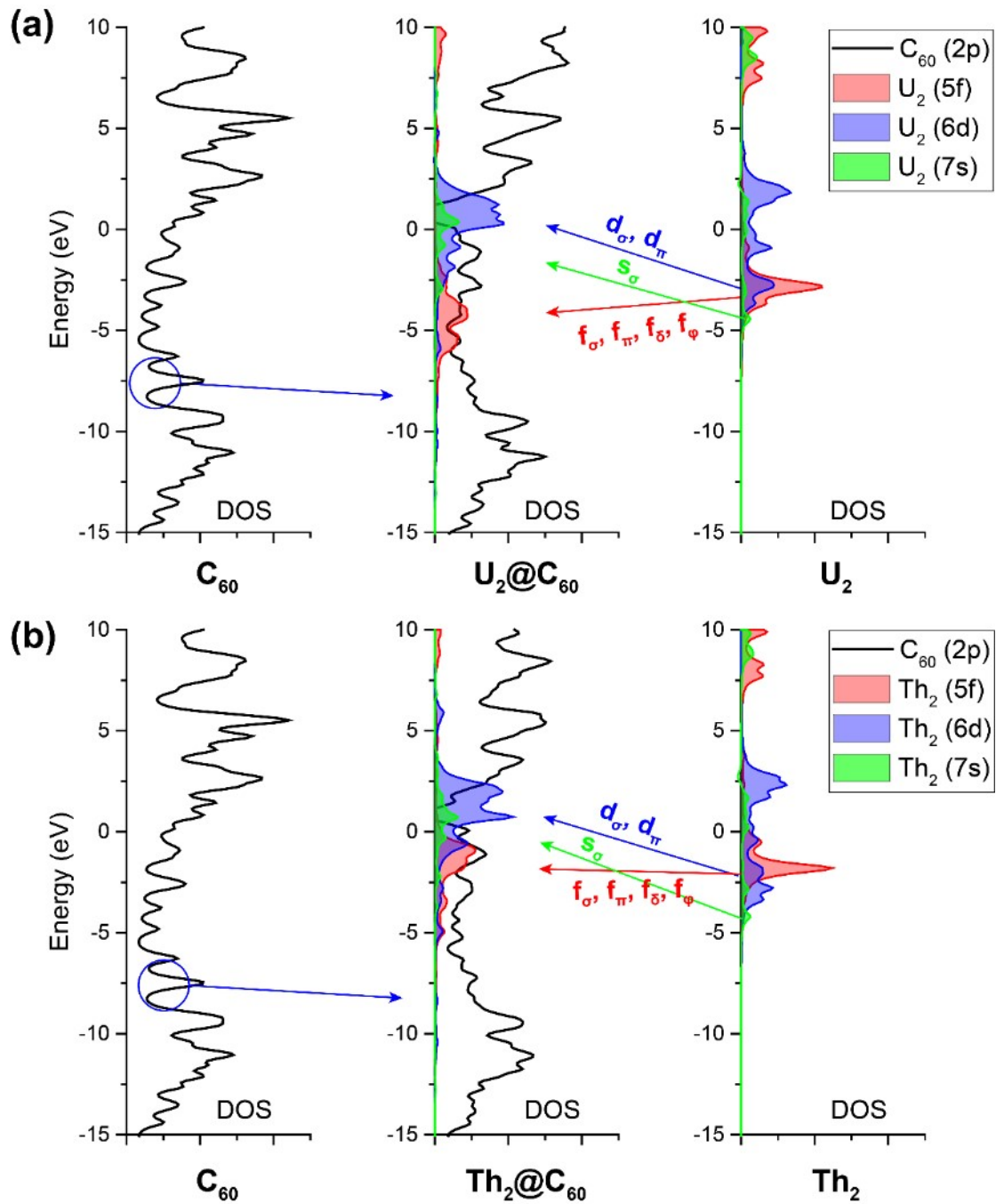


Fig. S27. Projected density of states (DOS). The left one shows the 2p orbitals (black line) of C atoms in C₆₀. The right one shows the 5f (red shadow), 6d (blue shadow), and 7s (green shadow) orbitals of M atoms in M₂. The middle one shows the shifts of the 2p orbitals of C atoms and the 5f, 6d, and 7s orbitals of M atoms in M₂@C₆₀. The green and blue arrows indicates that the s_σ, d_σ and d_π bonding orbitals become unoccupied in M₂@C₆₀, due to the strong orbital interaction with the C₆₀ orbitals.

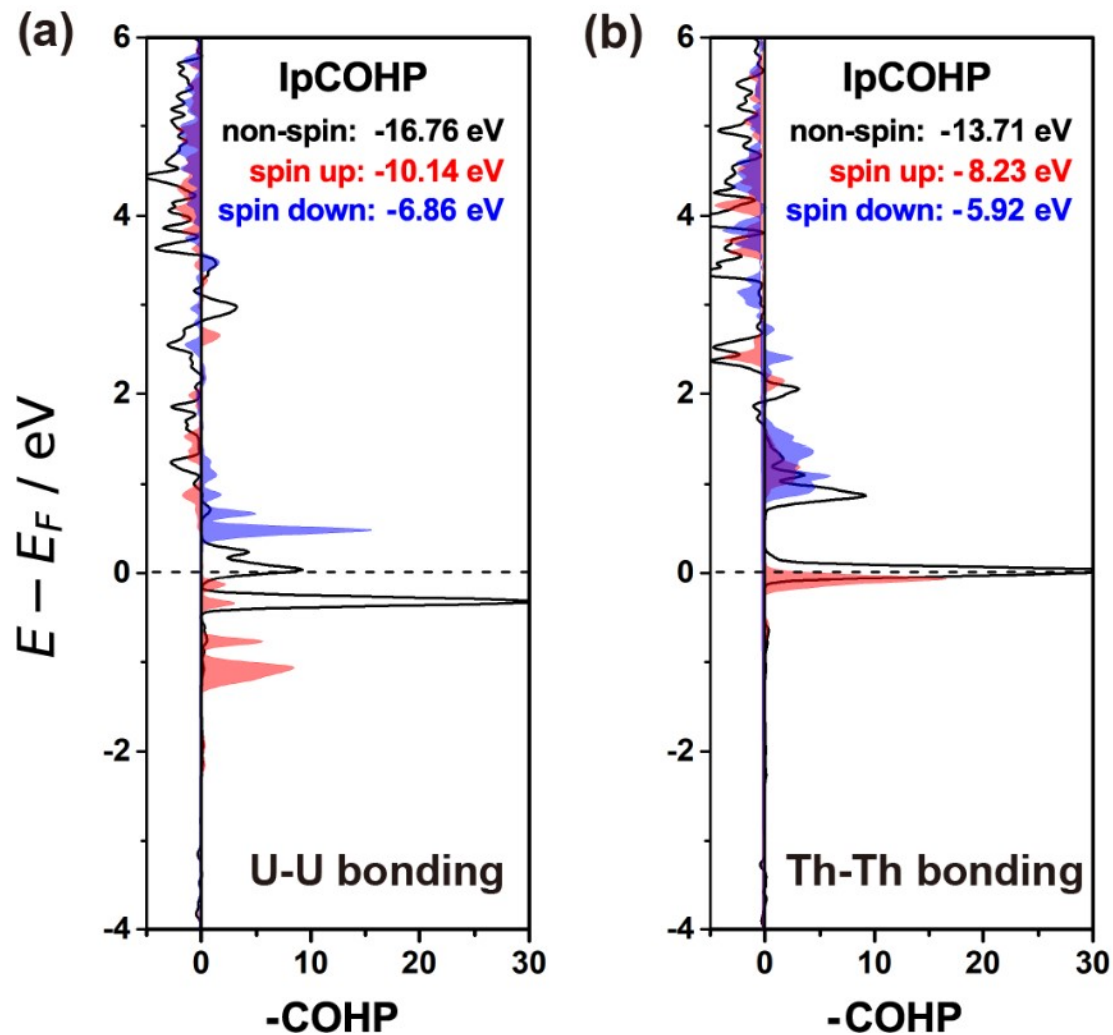


Fig. S28. Crystal orbital Hamilton populations (COHP) for **(a)** U–U bonding and **(b)** Th–Th bonding and their corresponding integrated values (IpCOHP). The non-spin-polarized COHP curves are marked by black lines. The spin-polarized COHP curves for spin up and spin down states are marked by red and blue areas, respectively.

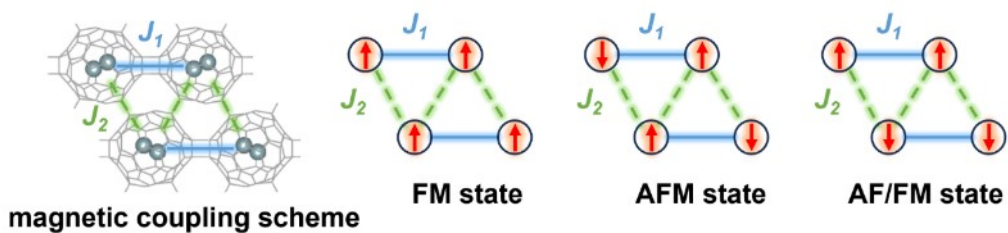


Fig. S29. The magnetic coupling scheme of the 2D actinide EMFs monolayers for ferromagnetic (FM), antiferromagnetic (AFM), and antiferromagnetic/ferromagnetic (AF/FM) states, respectively. The supercell model includes 8 U atoms and 240 C atoms in a unit cell. The red arrows represent the magnetic moment orientation of unpaired electrons in encapsulated M₂ dimers. The magnetic coupling along the interfullerene [2 + 2] cycloaddition bonds and C–C single bonds are indicated by the blue solid lines (J_1) and green dash lines (J_2), respectively.

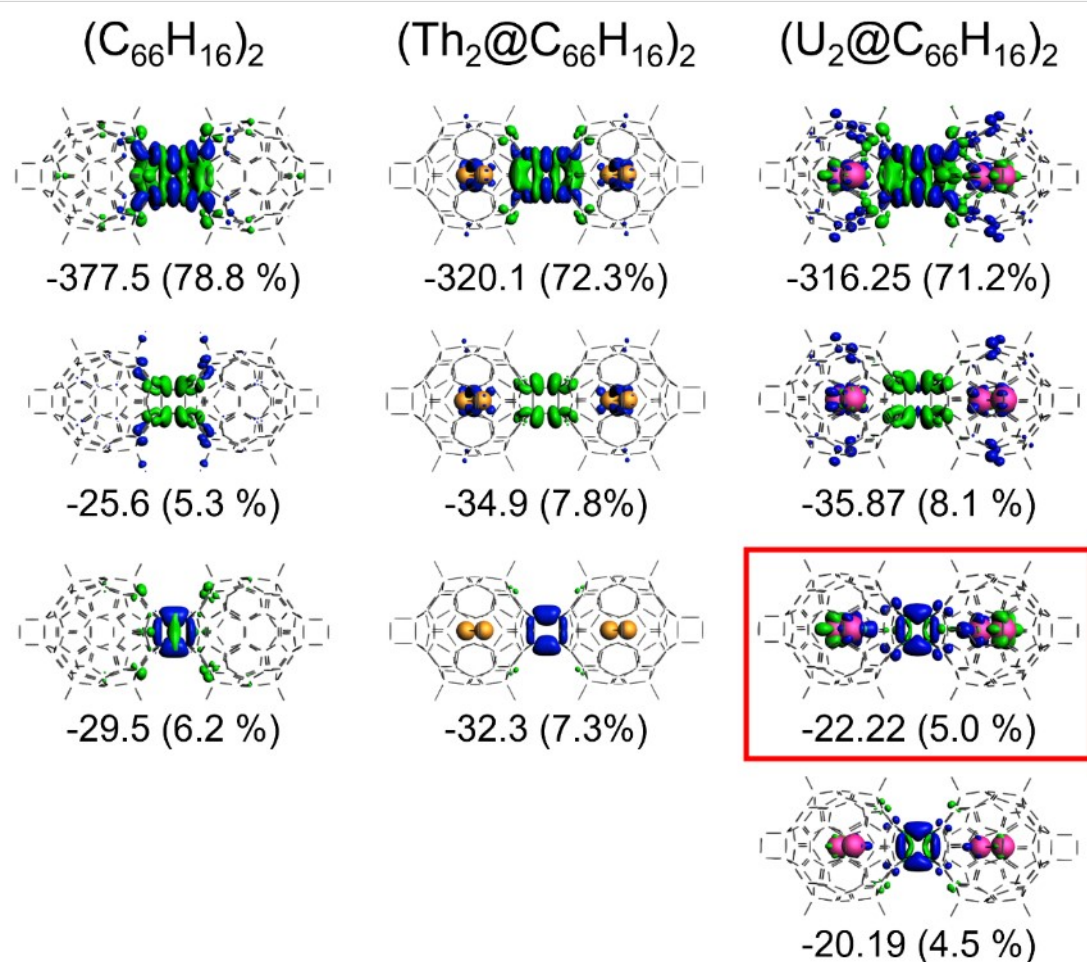


Fig. S30. Energy decomposition analysis (EDA) with NOCV extension of the molecular model for $(C_{66}H_{16})_2$, $(Th_2@C_{66}H_{16})_2$, and $(U_2@C_{66}H_{16})_2$ dimers at the BP86/TZP level, along with the associated deformation densities $\Delta\rho$ of the most important pairwise orbital interactions ΔE_{orb} (isosurfaces = 0.001 au). The direction of the charge flow is indicated from green to blue. Energy values are given in $\text{kcal}\cdot\text{mol}^{-1}$. The values in parentheses give the percentage contribution to the total orbital interaction (ΔE_{orb}). The NOCV orbital in the red box shows that the f orbitals of U_2 dimer contribute to the interactions between two EMF cages. See **Supplementary Tables 7–9** for more details on the EDA-NOCV analyses.

3. Supplementary Tables

Table S1. Comparison of bond lengths and integrated projected Crystal Orbital Hamilton Population (IpCOHP) of interfullerene C–C single bond and [2+2] cycloaddition bonds

	interfullerene bond	bond length (Å)	IpCOHP (eV)
2D qHPC ₆₀	C–C single bonds	1.606	-7.90
	[2+2] cycloaddition bonds	1.606	-7.89
U ₂ @C ₆₀ -2D	C–C single bonds	1.591	-8.49
	[2+2] cycloaddition bonds	1.618	-8.46
Th ₂ @C ₆₀ -2D	C–C single bonds	1.602	-8.03
	[2+2] cycloaddition bonds	1.613	-7.82

Table S2. The formation energy of 2D actinide endohedral metallofullerenes U₂@C₆₀-2D and Th₂@C₆₀-2D monolayers from 2D qHPC₆₀ monolayer and the most stable crystalline metal uranium and thorium at ambient temperature and pressure (300 K, 1 atm).

	E /eV	Correction /eV	Gibbs free energy /eV
U (bulk)	-11.137	-0.077	-11.214
Th (bulk)	-7.442	-0.097	-7.539
2D qHPC ₆₀	-1059.194	19.222	-1039.971
U ₂ @C ₆₀ -2D	-1104.143	18.793	-1085.350
Th ₂ @C ₆₀ -2D	-1087.504	18.661	-1068.843

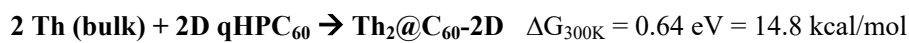


Table S3. The electronic energies of the 2D actinide endohedral metallofullerenes $\text{U}_2@\text{C}_{60}$ -2D and $\text{Th}_2@\text{C}_{60}$ -2D monolayers for ferromagnetic (FM) and antiferromagnetic (AFM) states in each EMF cage, respectively. The magnetic moments for FM states are listed as well. The calculation model includes two EMF cages (4 U atoms and 120 C atoms) in a unit cell.

	$\text{U}_2@\text{C}_{60}$ -2D	$\text{Th}_2@\text{C}_{60}$ -2D
FM (eV)	-1104.143	-1087.504
AFM (eV)	-1103.183	-1086.717
magnetic moments (μ_B)	2.75	0.68

$\text{U}_2@\text{C}_{60}$ -2D: $\Delta E = E_{\text{FM}} - E_{\text{AFM}} = -0.961 \text{ eV} = -22.10 \text{ kcal/mol}$

$\text{Th}_2@\text{C}_{60}$ -2D: $\Delta E = E_{\text{FM}} - E_{\text{AFM}} = -0.787 \text{ eV} = -18.09 \text{ kcal/mol}$

Table S4. The comparison of Bader charges and oxidation states for 2D actinide endohedral metallofullerenes of $\text{U}_2@\text{C}_{60}$ -2D and $\text{Th}_2@\text{C}_{60}$ -2D monolayers and other published actinide EMFs of $\text{U}_2\text{C}_2@\text{C}_{78}$, $\text{U}_2@\text{C}_{80}$, $\text{ThC}_2@\text{C}_{82}$ and $\text{Th}_2@\text{C}_{80}$.

	Bader charges of M (M = U, Th)	formal oxidation state
$\text{U}_2\text{C}_2@\text{C}_{78}$ ²²	2.00	+4
$\text{U}_2@\text{C}_{80}$ ²³	1.54	+3
$\text{U}_2@\text{C}_{60}$ -2D	1.45	+3
$\text{ThC}_2@\text{C}_{82}$ ²⁴	2.28	+4
$\text{Th}_2@\text{C}_{80}$ ²⁵	1.68	+3
$\text{Th}_2@\text{C}_{60}$ -2D	1.64	+3

Table S5. Computationally calculated relative electronic energies (ΔE , kcal/mol) of the $\text{U}_2@\text{C}_{66}\text{H}_{20}$ and $\text{Th}_2@\text{C}_{66}\text{H}_{20}$ molecule models for different multiplicity states at BP86/TZP and PBE0/TZP level.

Multiplicity	$\text{U}_2@\text{C}_{66}\text{H}_{20}$				$\text{Th}_2@\text{C}_{66}\text{H}_{20}$			
	ΔE (BP86)	$\langle S^2 \rangle$	ΔE (PBE0)	$\langle S^2 \rangle$	ΔE (BP86)	$\langle S^2 \rangle$	ΔE (PBE0)	$\langle S^2 \rangle$
1	13.31	0.00	20.44	0.00	16.56	0.00	17.77	0.00
3	8.95	2.03	10.09	3.42	0.00	2.01	0.00	2.01
5	6.07	6.06	3.94	7.37				
7	0.00	12.11	0.00	12.25				

The spin density of the U atom is 2.98 in septet $\text{U}_2@\text{C}_{66}\text{H}_{20}$.

The spin density of the Th atom is 0.96 in triplet $\text{Th}_2@\text{C}_{66}\text{H}_{20}$.

Table S6. The electronic energy of the 2D actinide endohedral metallofullerenes monolayers for ferromagnetic (FM), antiferromagnetic (AFM), and antiferromagnetic/ferromagnetic (AF/FM) states, respectively. The supercell model includes 8 U atoms and 240 C atoms in a unit cell, as shown in **Fig. S17**.

	FM (eV)	AFM (eV)	AF-FM (eV)
$\text{U}_2@\text{C}_{60}$ -2D	-2208.2614	-2208.4069	-2208.2658
$\text{Th}_2@\text{C}_{60}$ -2D	-2174.9873	-2174.9756	-2174.9765

$\text{U}_2@\text{C}_{60}$ -2D: $\Delta E = E_{\text{AFM}} - E_{\text{FM}} = -0.145 \text{ eV} = -3.36 \text{ kcal/mol}$

$\text{Th}_2@\text{C}_{60}$ -2D: $\Delta E = E_{\text{FM}} - E_{\text{AFM}} = -0.012 \text{ eV} = -0.27 \text{ kcal/mol}$

Table S7. Energy decomposition analysis (EDA) with NOCV extension of the molecular model ($C_{66}H_{16}$)₂ dimer at the BP86/TZP level and the associated deformation densities $\Delta\rho$ of the most important pairwise orbital interactions ΔE_{orb} (isosurfaces = 0.001 au). The direction of the charge flow is green to blue. Energy values are given in kcal·mol⁻¹.

	Fragment 1: $C_{66}H_{16}$ Fragment 2: $C_{66}H_{16}$			
ΔE_{int}	-107.09			
ΔE_{Pauli}	678.07			
$\Delta E_{\text{elstat}}^{\text{a}}$	-281.62 (35.9 %)			
$\Delta E_{\text{orb}}^{\text{a}}$	-478.94 (61.0 %)			
$\Delta E_{\text{disp}}^{\text{a}}$	-24.59 (3.1 %)			
	Energy	Donor orbitals	Acceptor orbitals	
$\Delta E_{\text{orb-1}}^{\text{b}}$	-377.5 (78.8 %)			
$\Delta E_{\text{orb-2}}^{\text{b}}$	-25.6 (5.3 %)			
$\Delta E_{\text{orb-3}}^{\text{b}}$	-29.5 (6.2 %)			

^a The values in parentheses give the percentage contribution to the total attractive interaction, $\Delta E_{\text{elstat}} + \Delta E_{\text{orb}} + \Delta E_{\text{disp}}$

^b The values in parentheses give the percentage contribution to the total orbital interaction, ΔE_{orb} .

Table S8. Energy decomposition analysis (EDA) with NOCV extension of the molecular model ($\text{Th}_2@\text{C}_{66}\text{H}_{16}$)₂ dimer at the BP86/TZP level and the associated deformation densities $\Delta\rho$ of the most important pairwise orbital interactions ΔE_{orb} (isosurfaces = 0.001 au). The direction of the charge flow is green to blue. Energy values are given in kcal·mol⁻¹.

		fragment 1: $\text{Th}_2@\text{C}_{66}\text{H}_{16}$ fragment 2: $\text{Th}_2@\text{C}_{66}\text{H}_{16}$			
ΔE_{int}		-96.82			
ΔE_{Pauli}		652.91			
$\Delta E_{\text{elstat}}^{\text{a}}$		-279.71 (37.3 %)			
$\Delta E_{\text{orb}}^{\text{a}}$		-442.78 (59.1 %)			
$\Delta E_{\text{disp}}^{\text{a}}$		-27.23 (3.6 %)			
		Energy	donor orbitals	acceptor orbitals	deformation densities
spin α	$\Delta E_{\text{orb-1}}^{\text{b}}$	-148.7 (33.6 %)			
	$\Delta E_{\text{orb-2}}^{\text{b}}$	-23.2 (5.2 %)			
	$\Delta E_{\text{orb-3}}^{\text{b}}$	-15.6 (3.5 %)			
spin β	$\Delta E_{\text{orb-1}}^{\text{b}}$	-171.4 (38.7 %)			
	$\Delta E_{\text{orb-2}}^{\text{b}}$	-11.7 (2.6 %)			
	$\Delta E_{\text{orb-3}}^{\text{b}}$	-16.7 (3.8 %)			

^a The values in parentheses give the percentage contribution to the total attractive interaction, $\Delta E_{\text{elstat}} + \Delta E_{\text{orb}} + \Delta E_{\text{disp}}$

^b The values in parentheses give the percentage contribution to the total orbital interaction, ΔE_{orb} .

Table S9. Energy decomposition analysis (EDA) with NOCV extension of the molecular model ($\text{U}_2@\text{C}_{66}\text{H}_{16}$)₂ dimer at the BP86/TZP level and the associated deformation densities $\Delta\rho$ of the most important pairwise orbital interactions ΔE_{orb} (isosurfaces = 0.001 au). The direction of the charge flow is green to blue. Energy values are given in kcal·mol⁻¹.

	fragment 1: $\text{U}_2@\text{C}_{66}\text{H}_{16}$ fragment 2: $\text{U}_2@\text{C}_{66}\text{H}_{16}$			
ΔE_{int}	-104.28			
ΔE_{Pauli}	639.30			
$\Delta E_{\text{elstat}}^{\text{a}}$	-273.41 (36.8 %)			
$\Delta E_{\text{orb}}^{\text{a}}$	-444.46 (59.8 %)			
$\Delta E_{\text{disp}}^{\text{a}}$	-25.71 (3.5 %)			
	Energy	donor orbitals	acceptor orbitals	
$\Delta E_{\text{orb-1}}^{\text{b}}$	-316.25 (71.2%)			
$\Delta E_{\text{orb-2}}^{\text{b}}$	-35.87 (8.1 %)			
$\Delta E_{\text{orb-3}}^{\text{b}}$	-22.22 (5.0 %)			
$\Delta E_{\text{orb-4}}^{\text{b}}$	-20.19 (4.5 %)			

^a The values in parentheses give the percentage contribution to the total attractive interaction, $\Delta E_{\text{elstat}} + \Delta E_{\text{orb}} + \Delta E_{\text{disp}}$

^b The values in parentheses give the percentage contribution to the total orbital interaction, ΔE_{orb} .

Table S10. The cartesian coordinate of optimized U₂@C₆₀-2D monolayer. (POSCAR format)

Primitive Cell

1.0

15.8948364258	0.0000000000	0.0000000000
0.0000000000	9.2410135269	0.0000000000
0.0000000000	0.0000000000	20.0000000000

C U

120 4

Cartesian

15.163506199	4.167824383	6.457072496
1.445575999	3.051158365	7.052248716
1.159964212	5.520203716	6.806865931
2.296874718	5.797989071	7.617508173
3.025431888	4.699785564	8.181311488
2.535482966	3.368397498	7.960658669
2.498643791	2.456122034	9.051157832
1.388508757	1.592256062	8.890455961
0.728751921	1.923819078	7.642195225
15.093544049	0.808164824	10.025594234
1.190192032	1.513184916	11.329702139
2.318151564	2.323825550	11.482521296
3.266551945	2.676807672	10.323766470
3.482408236	4.172751080	10.528137684
8.677908091	8.788330871	13.542926311
6.501000562	7.671664853	12.947751284
6.786613652	0.899696677	13.193132877
5.649702672	1.177482033	12.382490635
4.921145029	0.079278301	11.818687916
5.411093714	7.988903436	12.039341927
5.447933599	7.076628798	10.948841572
6.558068988	6.212762963	11.109544039
7.217825529	6.544325841	12.357804775
8.747869293	5.428671656	9.974406362
6.756385713	6.133691817	8.670296669
5.628426300	6.944332589	8.517478704
4.680025445	7.297314160	9.676233530
4.464169865	8.793257843	9.471861720
8.677908091	0.452682449	6.457072496
6.501000562	1.569348674	7.052248120
6.786613652	8.341317125	6.806865931
5.649702672	8.063530668	7.617508173
4.921145029	9.161735277	8.181311488
5.411093714	1.252109954	7.960658073

5.447933599	2.164385142	9.051157832
6.558068988	3.028250839	8.890455961
7.217825529	2.696687410	7.642195225
8.747869293	3.812341871	10.025594234
6.756385713	3.107321710	11.329702139
5.628426300	2.296680938	11.482520103
4.680025445	1.943699229	10.323766470
4.464169865	0.447755959	10.528137684
15.163506199	5.073189419	13.542927504
1.445575999	6.189854886	12.947751284
1.159964212	3.720810086	13.193134069
2.296874718	3.443024456	12.382490635
3.025431888	4.541228238	11.818687916
2.535482966	5.872616304	12.039340734
2.498643791	6.784891493	10.948841572
1.388508757	7.648757327	11.109542847
0.728751921	7.317194449	12.357804775
15.093544049	8.432849185	9.974406362
1.190192032	7.727828473	8.670296669
2.318151564	6.917188253	8.517478108
3.266551945	6.564206130	9.676233530
3.482408236	5.068262998	9.471861124
0.730489523	5.073189419	13.542926311
14.448419249	6.189855437	12.947751284
14.734031865	3.720810086	13.193132877
13.597120885	3.443024731	12.382490635
12.868563715	4.541228238	11.818687916
13.358511927	5.872616855	12.039341927
13.395351812	6.784891493	10.948841572
14.505487201	7.648757327	11.109544039
15.165243741	7.317194449	12.357804775
0.800451494	8.432849185	9.974406362
14.703803926	7.727828473	8.670296669
13.575844986	6.917187702	8.517478704
12.627443184	6.564206130	9.676233530
12.411588078	5.068262447	9.471861720
7.216087512	0.452682518	6.457072496
9.392994093	1.569348261	7.052248716
9.107382425	8.341316023	6.806865931
10.244293405	8.063530668	7.617508173
10.972850574	9.161734726	8.181311488
10.482901415	1.252109265	7.960658669
10.446061530	2.164384867	9.051157832
9.335927088	3.028250564	8.890455961

8.676170548	2.696687686	7.642195225
7.146125836	3.812341871	10.025594234
9.137610363	3.107321710	11.329702139
10.265569303	2.296681351	11.482521296
11.213970158	1.943699229	10.323766470
11.429826212	0.447755994	10.528137684
7.216087512	8.788330871	13.542927504
9.392994093	7.671665404	12.947751284
9.107382425	0.899696746	13.193134069
10.244293405	1.177482446	12.382490635
10.972850574	0.079278585	11.818687916
10.482901415	7.988903986	12.039340734
10.446061530	7.076628798	10.948841572
9.335927088	6.212762963	11.109542847
8.676170548	6.544325841	12.357804775
7.146125836	5.428671656	9.974406362
9.137610363	6.133691817	8.670296669
10.265569303	6.944332038	8.517478108
11.213970158	7.297314160	9.676233530
11.429826212	8.793257843	9.471861124
0.730489523	4.167824383	6.457072496
14.448419249	3.051158090	7.052248120
14.734031865	5.520203165	6.806865931
13.597120885	5.797989071	7.617508173
12.868563715	4.699785013	8.181311488
13.358511927	3.368396948	7.960658073
13.395351812	2.456121759	9.051157832
14.505487201	1.592256062	8.890455961
15.165243741	1.923819215	7.642195225
0.800451494	0.808164755	10.025594234
14.703803926	1.513185054	11.329702139
13.575844986	2.323825825	11.482520103
12.627443184	2.676807672	10.323766470
12.411588078	4.172751080	10.528137684
15.894416725	1.816386174	12.074438334
15.894415777	2.898784953	13.002936840
7.946998038	6.436893075	7.925561666
7.946998038	7.519291717	6.997061968
7.946998038	2.804120727	12.074438334
7.946998038	1.721721672	13.002936840
15.894416725	7.424627215	7.925561666
15.894415777	6.342228573	6.997061968
7.946996617	8.601894158	11.188385487
7.946996617	0.639118887	8.811613917

15.894414830	5.259625582	11.188385487
15.894414830	3.981387945	8.811613917

Table S11. The cartesian coordinate of optimized Th₂@C₆₀-2D monolayer. (POSCAR format)

Primitive Cell

1.0

15.8027591705	0.0000000000	0.0000000000
0.0000000000	9.1973381042	0.0000000000
0.0000000000	0.0000000000	20.0000000000

C Th

120 4

Cartesian

15.062447536	4.130939146	5.149889230
1.464661765	2.998033223	5.758493747
1.164436283	5.486544202	5.536670660
2.289426931	5.763500188	6.380393375
3.011773132	4.666733521	6.948976938
2.544722932	3.327094909	6.695074879
2.494542023	2.426112474	7.798690046
1.395342381	1.551084760	7.621345624
0.741605536	1.858499512	6.352630209
15.001810632	0.806523448	8.789240217
1.180986251	1.517472998	10.098803930
2.297888886	2.328305741	10.260696385
3.237485612	2.665154940	9.096851067
3.442043794	4.157225257	9.315484689
8.640854797	8.729608747	12.420406776
6.435880220	7.596700630	11.811808019
6.736105230	0.887876178	12.033633725
5.611116702	1.164832369	11.189909962
4.888772621	0.068065137	10.621323258
5.355819760	7.925762316	10.875225840
5.406000433	7.024778511	9.771612245
6.505200193	6.149752167	9.948955096
7.158938745	6.457168016	11.217669986
8.701490758	5.405192911	8.781059456
6.719558089	6.116140679	7.471494172
5.602655925	6.926974519	7.309600145
4.663061318	7.263822896	8.473448081
4.458509729	8.755895680	8.254817077
8.640854797	0.467729358	5.149891849
6.435880220	1.600637474	5.758491129
6.736105230	8.309461858	5.536665424
5.611116702	8.032505872	6.380389710
4.888772621	9.129273087	6.948976414
5.355819760	1.271575651	6.695073832

5.406000433	2.172559320	7.798686380
6.505200193	3.047586211	7.621344053
7.158938745	2.740170363	6.352629686
8.701490758	3.792145193	8.789240217
6.719558089	3.081197425	10.098804977
5.602655925	2.270363723	10.260698480
4.663061318	1.933515346	9.096851067
4.458509729	0.441442493	9.315481548
15.062447536	5.066398958	12.420409918
1.464661765	6.199304882	11.811804878
1.164436283	3.710794176	12.033628488
2.289426931	3.433838190	11.189905773
3.011773132	4.530604857	10.621322211
2.544722932	5.870243195	10.875224793
2.494542023	6.771225357	9.771609103
1.395342381	7.646253344	9.948953001
0.741605536	7.338838592	11.217668939
15.001810632	8.390814794	8.781058932
1.180986251	7.679864832	7.471495743
2.297888886	6.869032089	7.309602240
3.237485612	6.532183164	8.473448081
3.442043794	5.040113121	8.254813936
0.739475329	5.066398410	12.420406776
14.337260276	6.199306526	11.811808019
14.637484345	3.710792806	12.033633725
13.512496287	3.433836546	11.189909962
12.790152677	4.530604035	10.621323258
13.257199816	5.870244840	10.875225840
13.307379547	6.771228646	9.771612245
14.406579778	7.646254989	9.948955096
15.060317860	7.338839141	11.217669986
0.800111232	8.390814245	8.781059456
14.620937674	7.679866477	7.471494172
13.504035039	6.869032638	7.309600145
12.564440904	6.532184261	8.473448081
12.359889314	5.040111476	8.254817077
7.161067951	0.467729906	5.149889230
9.366041115	1.600635692	5.758493747
9.065816104	8.309462954	5.536670660
10.190806988	8.032506968	6.380393375
10.913152481	9.129273635	6.948976938
10.446102517	1.271574143	6.695074879
10.395921844	2.172556442	7.798690046
9.296721613	3.047584292	7.621345624

8.642985415	2.740169540	6.352630209
7.100430576	3.792145467	8.789240217
9.082365601	3.081196054	10.098803930
10.199268236	2.270363311	10.260696385
11.138865197	1.933513975	9.096851067
11.343423380	0.441443863	9.315484689
7.161067951	8.729608198	12.420409918
9.366041115	7.596702275	11.811804878
9.065816104	0.887874876	12.033628488
10.190806988	1.164830999	11.189905773
10.913152481	0.068064229	10.621322211
10.446102517	7.925763961	10.875224793
10.395921844	7.024781800	9.771609103
9.296721613	6.149753812	9.948953001
8.642985415	6.457168564	11.217668939
7.100430576	5.405192363	8.781058932
9.082365601	6.116142324	7.471495743
10.199268236	6.926975067	7.309602240
11.138865197	7.263823992	8.473448081
11.343423380	8.755894035	8.254813936
0.739475329	4.130939694	5.149891849
14.337260276	2.998031578	5.758491129
14.637484345	5.486545299	5.536665424
13.512496287	5.763501284	6.380389710
12.790152677	4.666734070	6.948976414
13.257199816	3.327093264	6.695073832
13.307379547	2.426109733	7.798686380
14.406579778	1.551082978	7.621344053
15.060317860	1.858498827	6.352629686
0.800111232	0.806523927	8.789240217
14.620937674	1.517471764	10.098804977
13.504035039	2.328305192	10.260698480
12.564440904	2.665153843	9.096851067
12.359889314	4.157226628	9.315481548
15.802340959	1.826341724	10.856861936
15.802340959	2.890048807	11.819233174
7.900961374	6.425010913	6.713437737
7.900961374	7.488718133	5.751066498
7.900961374	2.772327465	10.856861936
7.900961374	1.708620245	11.819233174
15.802340959	7.370996243	6.713437737
15.802340959	6.307289023	5.751066498
7.900951484	8.545962028	10.054953627
7.900951484	0.651375940	7.515346045

15.802330598	5.250045129	10.054953627
15.802330598	3.947293250	7.515346045

Table S12. The cartesian coordinate of optimized U₂@C₆₆H₂₀ cluster model. (XYZ format)

C	8.67848000	8.78851000	12.32770000
C	6.50142000	7.67199000	11.73270000
C	5.41139000	7.98901000	10.82450000
C	5.44814000	7.07670000	9.73407000
C	6.55827000	6.21275000	9.89478000
C	7.21828000	6.54435000	11.14300000
C	8.74845000	5.42907000	8.75960000
C	6.75679000	6.13398000	7.45550000
C	5.62858000	6.94419000	7.30246000
C	4.67986000	7.29719000	8.46151000
C	4.46422000	8.79336000	8.25697000
C	6.78702000	8.34147000	5.59219000
C	5.64993000	8.06358000	6.40258000
C	4.92151000	9.16173000	6.96662000
C	8.74845000	3.81208000	8.81070000
C	3.26724000	6.56455000	8.46151000
C	12.62780000	6.56455000	8.46151000
C	9.10803000	8.34147000	5.59219000
C	10.24510000	8.06358000	6.40258000
C	10.97350000	9.16173000	6.96662000
C	7.14661000	3.81208000	8.81070000
C	7.21658000	8.78851000	12.32770000
C	9.39363000	7.67199000	11.73270000
C	10.48370000	7.98901000	10.82450000
C	10.44690000	7.07670000	9.73407000
C	9.33679000	6.21275000	9.89478000
C	8.67678000	6.54435000	11.14300000
C	7.14661000	5.42907000	8.75960000
C	9.13827000	6.13398000	7.45550000
C	10.26650000	6.94419000	7.30246000
C	11.21520000	7.29719000	8.46151000
C	11.43080000	8.79336000	8.25697000
C	7.94754000	6.43721000	6.71071000
C	7.94754000	7.51947000	5.78235000
U	7.94752000	8.60092000	9.97227000
C	3.26724000	11.91780000	9.10879000
C	6.78702000	10.14090000	11.97810000
C	5.64993000	10.41870000	11.16770000
C	4.92151000	9.32059000	10.60370000

C	8.74845000	14.67020000	8.75960000
C	8.67848000	9.69381000	5.24259000
C	6.50142000	10.81030000	5.83761000
C	5.41139000	10.49330000	6.74584000
C	5.44814000	11.40560000	7.83623000
C	6.55827000	12.26960000	7.67552000
C	7.21828000	11.93800000	6.42727000
C	8.74845000	13.05320000	8.81070000
C	6.75679000	12.34830000	10.11480000
C	5.62858000	11.53810000	10.26780000
C	4.67986000	11.18510000	9.10879000
C	4.46422000	9.68896000	9.31333000
C	7.21658000	9.69381000	5.24259000
C	9.39363000	10.81030000	5.83761000
C	10.48370000	10.49330000	6.74584000
C	10.44690000	11.40560000	7.83623000
C	9.33679000	12.26960000	7.67552000
C	8.67678000	11.93800000	6.42727000
C	7.14661000	13.05320000	8.81070000
C	9.13827000	12.34830000	10.11480000
C	10.26650000	11.53810000	10.26780000
C	11.21520000	11.18510000	9.10879000
C	11.43080000	9.68896000	9.31333000
C	9.10803000	10.14090000	11.97810000
C	10.24510000	10.41870000	11.16770000
C	10.97350000	9.32059000	10.60370000
C	7.14661000	14.67020000	8.75960000
C	12.62780000	11.91780000	9.10879000
C	7.94754000	12.04510000	10.85960000
C	7.94754000	10.96290000	11.78790000
U	7.94752000	9.88140000	7.59803000
H	9.18290000	3.40818000	9.78421000
H	9.28585000	3.40287000	7.89236000
H	3.39944000	5.48428000	8.80084000
H	2.83045000	6.58138000	7.40864000
H	2.55985000	7.10313000	9.17504000
H	13.06460000	6.58138000	7.40864000
H	12.49560000	5.48428000	8.80084000
H	13.33520000	7.10313000	9.17504000
H	6.71216000	3.40818000	9.78421000
H	6.76661000	3.24555000	7.89733000
H	2.46038000	11.18740000	9.44813000
H	3.02938000	12.28450000	8.05593000
H	3.29998000	12.80630000	9.82233000

H	9.18290000	15.07410000	7.78609000
H	9.28585000	15.07940000	9.67794000
H	6.71216000	15.13480000	9.70567000
H	6.60920000	15.02060000	7.81726000
H	12.86570000	12.28450000	8.05593000
H	13.43470000	11.18740000	9.44813000
H	12.59510000	12.80630000	9.82233000

Table S13. The cartesian coordinate of optimized Th₂@C₆₆H₂₀ cluster model. (XYZ format)

C	15.00140000	8.39088000	8.78924000
C	16.60230000	8.39088000	8.78924000
C	15.06200000	14.26380000	5.14975000
C	15.06200000	13.32850000	12.42060000
C	14.33680000	12.19550000	11.81190000
C	14.33680000	15.39680000	5.75844000
C	14.63700000	14.68410000	12.03370000
C	14.63700000	12.90820000	5.53663000
C	13.51210000	14.96100000	11.19000000
C	13.51210000	12.63130000	6.38034000
C	12.78970000	13.86420000	10.62140000
C	12.78970000	13.72810000	6.94886000
C	13.25680000	12.52470000	10.87520000
C	13.25680000	15.06770000	6.69513000
C	13.30700000	11.62370000	9.77156000
C	13.30700000	15.96870000	7.79874000
C	14.40620000	10.74860000	9.94894000
C	14.40620000	16.84370000	7.62136000
C	15.05980000	11.05590000	11.21770000
C	15.05980000	16.53650000	6.35258000
C	15.00140000	17.58830000	8.78924000
C	15.00140000	10.00400000	8.78106000
C	14.62050000	10.71490000	7.47152000
C	14.62050000	16.87740000	10.09880000
C	13.50360000	11.52580000	7.30958000
C	13.50360000	16.06650000	10.26070000
C	12.56420000	11.86260000	8.47344000
C	11.13860000	16.46130000	9.09686000
C	11.13860000	11.13100000	8.47344000
C	12.56420000	15.72970000	9.09686000
C	12.35970000	13.35470000	8.25481000
C	12.35970000	14.23760000	9.31549000
C	16.54170000	13.32850000	12.42060000
C	16.54170000	14.26380000	5.14975000

C	17.26690000	15.39680000	5.75844000
C	17.26690000	12.19550000	11.81190000
C	16.96670000	12.90820000	5.53663000
C	16.96670000	14.68410000	12.03370000
C	18.09160000	12.63130000	6.38034000
C	18.09160000	14.96100000	11.19000000
C	18.81400000	13.72810000	6.94886000
C	18.81400000	13.86420000	10.62140000
C	18.34680000	15.06770000	6.69513000
C	18.34680000	12.52470000	10.87520000
C	18.29660000	15.96870000	7.79874000
C	18.29660000	11.62370000	9.77156000
C	17.19750000	16.84370000	7.62136000
C	17.19750000	10.74860000	9.94894000
C	16.54380000	16.53650000	6.35258000
C	16.54380000	11.05590000	11.21770000
C	16.60230000	10.00400000	8.78106000
C	16.60230000	17.58830000	8.78924000
C	16.98320000	16.87740000	10.09880000
C	16.98320000	10.71490000	7.47152000
C	18.10010000	16.06650000	10.26070000
C	18.10010000	11.52580000	7.30958000
C	19.03950000	15.72970000	9.09686000
C	20.46510000	11.13100000	8.47344000
C	20.46510000	16.46130000	9.09686000
C	19.03950000	11.86260000	8.47344000
C	19.24390000	14.23760000	9.31549000
C	19.24390000	13.35470000	8.25481000
C	15.80180000	16.56860000	10.85690000
C	15.80180000	11.02370000	6.71340000
C	15.80180000	15.50490000	11.81930000
C	15.80180000	12.08740000	5.75095000
Th	15.80180000	14.44770000	7.51482000
Th	15.80180000	13.14460000	10.05550000
C	15.00140000	19.20140000	8.78106000
C	16.60230000	19.20140000	8.78106000
H	14.56690000	7.95157000	7.83119000
H	14.46400000	8.01561000	9.72197000
H	14.56690000	19.63100000	7.81859000
H	14.62140000	19.74360000	9.70912000
H	17.03680000	19.64080000	9.73911000
H	16.98230000	19.73410000	7.84753000
H	17.03680000	7.96132000	9.75171000
H	17.13970000	8.00616000	7.86038000

H	10.33470000	15.72720000	9.43508000
H	10.89970000	16.82810000	8.04424000
H	11.16720000	17.34930000	9.81127000
H	11.26630000	10.04980000	8.81165000
H	10.70130000	11.15070000	7.42081000
H	10.43390000	11.67190000	9.18784000
H	20.90230000	11.15070000	7.42081000
H	20.33730000	10.04980000	8.81165000
H	21.16980000	11.67190000	9.18784000
H	20.70400000	16.82810000	8.04424000
H	21.26900000	15.72720000	9.43508000
H	20.43650000	17.34930000	9.81127000

Table S14. The cartesian coordinate of optimized ($C_{66}H_{20}$)₂ dimer model. (XYZ format)

C	7.23510000000000	8.76445000000000	5.30544000000000
C	8.67980000000000	8.76445000000000	5.30544000000000
C	9.36837000000000	7.68579000000000	5.87976000000000
C	6.54653000000000	7.68579000000000	5.87976000000000
C	6.79194000000000	8.20431000000000	12.00820000000000
C	9.12296000000000	8.20431000000000	12.00820000000000
C	5.67724000000000	7.97345000000000	11.18730000000000
C	10.23770000000000	7.97345000000000	11.18730000000000
C	4.96924000000000	9.09686000000000	10.62090000000000
C	10.94570000000000	9.09686000000000	10.62090000000000
C	10.51510000000000	7.92561000000000	6.70936000000000
C	5.39978000000000	7.92561000000000	6.70936000000000
C	10.49550000000000	6.95260000000000	7.79698000000000
C	5.41937000000000	6.95260000000000	7.79698000000000
C	9.40103000000000	6.12816000000000	7.66005000000000
C	6.51387000000000	6.12816000000000	7.66005000000000
C	8.65037000000000	6.57511000000000	6.48254000000000
C	7.26453000000000	6.57511000000000	6.48254000000000
C	8.76260000000000	3.77804000000000	8.77830000000000
C	7.15230000000000	5.38438000000000	8.79200000000000
C	8.76260000000000	5.38438000000000	8.79200000000000
C	7.15230000000000	3.77804000000000	8.77830000000000
C	9.14260000000000	6.08185000000000	10.09330000000000
C	6.77230000000000	6.08185000000000	10.09330000000000
C	10.26510000000000	6.87447000000000	10.25060000000000
C	5.64979000000000	6.87447000000000	10.25060000000000
C	3.25585000000000	6.52201000000000	9.09259000000000
C	11.21330000000000	7.22163000000000	9.09259000000000

C	4.701600000000000	7.221630000000000	9.092590000000000
C	12.659000000000000	6.522010000000000	9.092590000000000
C	11.403300000000000	8.718110000000000	9.298920000000000
C	4.511590000000000	8.718110000000000	9.298920000000000
C	7.957450000000000	6.361200000000000	10.868900000000000
C	7.957450000000000	7.372200000000000	11.845200000000000
C	8.679800000000000	9.560410000000000	12.264900000000000
C	7.235100000000000	17.926900000000000	5.305440000000000
C	8.679800000000000	17.926900000000000	5.305440000000000
C	7.235100000000000	9.560410000000000	12.264900000000000
C	6.546530000000000	10.639100000000000	11.690500000000000
C	9.368370000000000	16.848200000000000	5.879760000000000
C	6.546530000000000	16.848200000000000	5.879760000000000
C	9.368370000000000	10.639100000000000	11.690500000000000
C	6.791940000000000	17.366700000000000	12.008200000000000
C	9.122960000000000	10.120500000000000	5.562050000000000
C	6.791940000000000	10.120500000000000	5.562050000000000
C	9.122960000000000	17.366700000000000	12.008200000000000
C	5.677240000000000	17.135900000000000	11.187300000000000
C	10.237700000000000	10.351400000000000	6.383030000000000
C	5.677240000000000	10.351400000000000	6.383030000000000
C	10.237700000000000	17.135900000000000	11.187300000000000
C	4.969240000000000	18.259300000000000	10.620900000000000
C	10.945700000000000	9.227990000000000	6.949390000000000
C	4.969240000000000	9.227990000000000	6.949390000000000
C	10.945700000000000	18.259300000000000	10.620900000000000
C	5.399780000000000	10.399200000000000	10.860900000000000
C	10.515100000000000	17.088000000000000	6.709360000000000
C	5.399780000000000	17.088000000000000	6.709360000000000
C	10.515100000000000	10.399200000000000	10.860900000000000
C	5.419370000000000	11.372300000000000	9.773320000000000
C	10.495500000000000	16.115000000000000	7.796980000000000
C	5.419370000000000	16.115000000000000	7.796980000000000
C	10.495500000000000	11.372300000000000	9.773320000000000
C	6.513870000000000	12.196700000000000	9.910250000000000
C	9.401030000000000	15.290600000000000	7.660050000000000
C	6.513870000000000	15.290600000000000	7.660050000000000
C	9.401030000000000	12.196700000000000	9.910250000000000
C	7.264530000000000	11.749700000000000	11.087800000000000
C	8.650370000000000	15.737500000000000	6.482540000000000
C	7.264530000000000	15.737500000000000	6.482540000000000
C	8.650370000000000	11.749700000000000	11.087800000000000
C	8.762600000000000	12.940500000000000	8.778300000000000
C	7.152300000000000	14.546800000000000	8.792000000000000

C	8.762600000000000	14.54680000000000	8.79200000000000
C	7.152300000000000	12.94050000000000	8.77830000000000
C	6.772300000000000	12.24300000000000	7.47704000000000
C	9.142600000000000	15.24430000000000	10.09330000000000
C	6.772300000000000	15.24430000000000	10.09330000000000
C	9.142600000000000	12.24300000000000	7.47704000000000
C	5.649790000000000	11.45040000000000	7.31968000000000
C	10.265100000000000	16.03690000000000	10.25060000000000
C	5.649790000000000	16.03690000000000	10.25060000000000
C	10.265100000000000	11.45040000000000	7.31968000000000
C	3.255850000000000	15.68440000000000	9.09259000000000
C	12.659000000000000	11.80280000000000	8.47770000000000
C	4.701600000000000	11.10320000000000	8.47770000000000
C	11.213300000000000	16.38410000000000	9.09259000000000
C	4.701600000000000	16.38410000000000	9.09259000000000
C	11.213300000000000	11.10320000000000	8.47770000000000
C	3.255850000000000	11.80280000000000	8.47770000000000
C	12.659000000000000	15.68440000000000	9.09259000000000
C	4.511590000000000	9.60674000000000	8.27138000000000
C	11.403300000000000	17.88050000000000	9.29892000000000
C	4.511590000000000	17.88050000000000	9.29892000000000
C	11.403300000000000	9.60674000000000	8.27138000000000
C	7.957450000000000	11.96370000000000	6.70142000000000
C	7.957450000000000	15.52360000000000	10.86890000000000
C	7.957450000000000	10.95270000000000	5.72507000000000
C	7.957450000000000	16.53460000000000	11.84520000000000
C	8.679800000000000	18.72280000000000	12.26490000000000
C	7.235100000000000	18.72280000000000	12.26490000000000
C	6.546530000000000	19.80150000000000	11.69050000000000
C	9.368370000000000	19.80150000000000	11.69050000000000
C	9.122960000000000	19.28300000000000	5.56205000000000
C	6.791940000000000	19.28300000000000	5.56205000000000
C	10.237700000000000	19.51380000000000	6.38303000000000
C	5.677240000000000	19.51380000000000	6.38303000000000
C	10.945700000000000	18.39040000000000	6.94939000000000
C	4.969240000000000	18.39040000000000	6.94939000000000
C	5.399780000000000	19.56170000000000	10.86090000000000
C	10.515100000000000	19.56170000000000	10.86090000000000
C	5.419370000000000	20.53470000000000	9.77332000000000
C	10.495500000000000	20.53470000000000	9.77332000000000
C	6.513870000000000	21.35910000000000	9.91025000000000
C	9.401030000000000	21.35910000000000	9.91025000000000
C	7.264530000000000	20.91220000000000	11.08780000000000
C	8.650370000000000	20.91220000000000	11.08780000000000

C	8.762600000000000	22.102900000000000	8.778300000000000
C	7.152300000000000	23.709200000000000	8.792000000000000
C	8.762600000000000	23.709200000000000	8.792000000000000
C	7.152300000000000	22.102900000000000	8.778300000000000
C	6.772300000000000	21.405400000000000	7.477040000000000
C	9.142600000000000	21.405400000000000	7.477040000000000
C	5.649790000000000	20.612800000000000	7.319680000000000
C	10.265100000000000	20.612800000000000	7.319680000000000
C	12.659000000000000	20.965300000000000	8.477700000000000
C	4.701600000000000	20.265600000000000	8.477700000000000
C	11.213300000000000	20.265600000000000	8.477700000000000
C	3.255850000000000	20.965300000000000	8.477700000000000
C	4.511590000000000	18.769200000000000	8.271380000000000
C	11.403300000000000	18.769200000000000	8.271380000000000
C	7.957450000000000	21.126100000000000	6.701420000000000
C	7.957450000000000	20.115100000000000	5.725070000000000
H	9.23002948356953	3.34186174616547	9.66966129163459
H	9.20769049385261	3.36928400168196	7.86237717428592
H	6.68511040153339	3.34192136284065	9.66984350244977
H	6.70703055810355	3.36917314037437	7.86252452383194
H	2.72456312227813	6.78781383724920	10.01670971725096
H	2.70143123030974	6.88660889428628	8.21861818277334
H	3.38343339515770	5.43334647303489	9.03209080282214
H	13.15762670303265	6.71964325454031	10.05177724181434
H	12.53667636593431	5.44090768653617	8.94681513289712
H	13.24350654390915	6.94841642259259	8.26815930547346
H	2.72022851378305	15.99339271011746	8.18673916676609
H	3.39094693320172	14.59820903041317	9.10438253752283
H	2.70161172581542	15.99456525035356	9.98807046113587
H	13.18976373092040	11.50415395851688	9.39064940508069
H	13.21801246160413	11.48231927255100	7.58799440316608
H	12.52405866577712	12.88913834520072	8.45127410290746
H	2.71036276765673	11.47022048332703	9.36973068238727
H	3.39078713197222	12.88853177127741	8.49565851228523
H	2.71217408901934	11.51429689413561	7.56790040601137
H	13.22706955629725	16.02102500636305	9.97099034204652
H	12.52326832419191	14.59981992420729	9.13958390570067
H	13.18147711027707	15.96568128766234	8.16995931253951
H	6.68517070042823	24.14520638273470	7.90035419573671
H	6.70692953509882	24.11811941925222	9.70767680211850
H	9.20804596406905	24.11811503809567	9.70763948046531
H	9.22966004582439	24.14523111553128	7.90032966519406
H	12.53340266608460	22.05468980898227	8.54424202262079
H	13.21522734471434	20.59742129356489	9.34833830463111

H	13.18888277041432	20.70261597151312	7.55269583605794
H	3.37895802729760	22.04959533726858	8.59836858484160
H	2.74612826335310	20.74549847859644	7.52969245778149
H	2.68044682381017	20.55732529688314	9.31872486617977

Reference

- (1) Kresse, G.; Joubert, D. From Ultrasoft Pseudopotentials to the Projector Augmented-Wave Method. *Phys. Rev. B* **1999**, *59* (3), 1758–1775. <https://doi.org/10.1103/PhysRevB.59.1758>.
- (2) Shields, A. E.; Santos-Carballal, D.; De Leeuw, N. H. A Density Functional Theory Study of Uranium-Doped Thoria and Uranium Adatoms on the Major Surfaces of Thorium Dioxide. *J. Nucl. Mater.* **2016**, *473*, 99–111. <https://doi.org/10.1016/j.jnucmat.2016.02.009>.
- (3) Heyd, J.; Scuseria, G. E.; Ernzerhof, M. Hybrid Functionals Based on a Screened Coulomb Potential. *J. Chem. Phys.* **2003**, *118* (18), 8207–8215.
- (4) Ehrlich, S.; Moellmann, J.; Reckien, W.; Bredow, T.; Grimme, S. System-Dependent Dispersion Coefficients for the DFT-D3 Treatment of Adsorption Processes on Ionic Surfaces. *Comput. Phys. Commun.* **2011**, *12* (17), 3414–3420.
- (5) Deringer, V. L.; Tchougréeff, A. L.; Dronskowski, R. Crystal Orbital Hamilton Population (COHP) Analysis As Projected from Plane-Wave Basis Sets. *J. Phys. Chem. A* **2011**, *115* (21), 5461–5466. <https://doi.org/10.1021/jp202489s>.
- (6) VandeVondele, J.; Krack, M.; Mohamed, F.; Parrinello, M.; Chassaing, T.; Hutter, J. Quickstep: Fast and Accurate Density Functional Calculations Using a Mixed Gaussian and Plane Waves Approach. *Comput. Phys. Commun.* **2005**, *167* (2), 103–128.
- (7) VandeVondele, J.; Hutter, J. Gaussian Basis Sets for Accurate Calculations on Molecular Systems in Gas and Condensed Phases. *J. Chem. Phys.* **2007**, *127* (11), 114105. <https://doi.org/10.1063/1.2770708>.
- (8) Lu, J.-B.; Cantu, D. C.; Xu, C.-Q.; Nguyen, M.-T.; Hu, H.-S.; Glezakou, V.-A.; Rousseau, R.; Li, J. Norm-Conserving Pseudopotentials and Basis Sets to Explore Actinide Chemistry in Complex Environments. *J. Chem. Theory Comput.* **2021**, *17* (6), 3360–3371. <https://doi.org/10.1021/acs.jctc.1c00026>.
- (9) Nosé, S. A Unified Formulation of the Constant Temperature Molecular Dynamics Methods. *J. Chem. Phys.* **1984**, *81* (1), 511–519.
- (10) Hoover, W. G. Canonical Dynamics: Equilibrium Phase-Space Distributions. *Phys. Rev. A* **1985**, *31* (3), 1695.
- (11) Te Velde, G.; Bickelhaupt, F. M.; Baerends, E. J.; Fonseca Guerra, C.; van Gisbergen, S. J.; Snijders, J. G.; Ziegler, T. Chemistry with ADF. *J. Comput. Chem.* **2001**, *22* (9), 931–967.
- (12) van Lenthe, E.; Baerends, E.-J.; Snijders, J. G. Relativistic Regular Two-component Hamiltonians. *J. Chem. Phys.* **1993**, *99* (6), 4597–4610.
- (13) van Lenthe, E.; Baerends, E.-J. Optimized Slater-type Basis Sets for the Elements 1–118. *J. Comput. Chem.* **2003**, *24* (9), 1142–1156.
- (14) Adamo, C.; Barone, V. Toward Reliable Density Functional Methods without Adjustable Parameters: The PBE0 Model. *J. Chem. Phys.* **1999**, *110* (13), 6158–6170. <https://doi.org/10.1063/1.478522>.
- (15) Neese, F. Software Update: The ORCA Program System—Version 5.0. *WIREs Comput. Mol. Sci.* **2022**, *12* (5), e1606. <https://doi.org/10.1002/wcms.1606>.
- (16) Pantazis, D. A.; Chen, X.-Y.; Landis, C. R.; Neese, F. All-Electron Scalar Relativistic Basis Sets for

- Third-Row Transition Metal Atoms. *J. Chem. Theory Comput.* **2008**, *4* (6), 908–919. <https://doi.org/10.1021/ct800047t>.
- (17) Weigend, F.; Ahlrichs, R. Balanced Basis Sets of Split Valence, Triple Zeta Valence and Quadruple Zeta Valence Quality for H to Rn: Design and Assessment of Accuracy. *Phys. Chem. Chem. Phys.* **2005**, *7* (18), 3297–3305. <https://doi.org/10.1039/B508541A>.
- (18) Zhao, L.; von Hopffgarten, M.; Andrada, D. M.; Frenking, G. Energy Decomposition Analysis. *WIREs Comput Mol Sci* **2018**, *8* (3), e1345. <https://doi.org/10.1002/wcms.1345>.
- (19) Zhang, J.-X.; Sheong, F. K.; Lin, Z. Unravelling Chemical Interactions with Principal Interacting Orbital Analysis. *Chem. Eur. J.* **2018**, *24* (38), 9639–9650. <https://doi.org/10.1002/chem.201801220>.
- (20) Frisch, M. J.; Trucks, G. W.; Schlegel, H. B.; Scuseria, G. E.; Robb, M. A.; Cheeseman, J. R.; Scalmani, G.; Barone, V.; Petersson, G. A.; Nakatsuji, H.; Li, X.; Caricato, M.; Marenich, A. V.; Bloino, J.; Janesko, B. G.; Gomperts, R.; Mennucci, B.; Hratchian, H. P.; Ortiz, J. V.; Izmaylov, A. F.; Sonnenberg, J. L.; Williams, Ding, F.; Lipparini, F.; Egidi, F.; Goings, J.; Peng, B.; Petrone, A.; Henderson, T.; Ranasinghe, D.; Zakrzewski, V. G.; Gao, J.; Rega, N.; Zheng, G.; Liang, W.; Hada, M.; Ehara, M.; Toyota, K.; Fukuda, R.; Hasegawa, J.; Ishida, M.; Nakajima, T.; Honda, Y.; Kitao, O.; Nakai, H.; Vreven, T.; Throssell, K.; Montgomery Jr., J. A.; Peralta, J. E.; Ogliaro, F.; Bearpark, M. J.; Heyd, J. J.; Brothers, E. N.; Kudin, K. N.; Staroverov, V. N.; Keith, T. A.; Kobayashi, R.; Normand, J.; Raghavachari, K.; Rendell, A. P.; Burant, J. C.; Iyengar, S. S.; Tomasi, J.; Cossi, M.; Millam, J. M.; Klene, M.; Adamo, C.; Cammi, R.; Ochterski, J. W.; Martin, R. L.; Morokuma, K.; Farkas, O.; Foresman, J. B.; Fox, D. J. Gaussian 16 Rev. C.01, 2016.
- (21) Moritz, A.; Dolg, M. Quasirelativistic Energy-Consistent 5f-in-Core Pseudopotentials for Pentavalent and Hexavalent Actinide Elements. *Theor. Chem. Acc.* **2008**, *121* (5), 297–306. <https://doi.org/10.1007/s00214-008-0477-9>.
- (22) Zhuang, J.; Abella, L.; Sergentu, D. C.; Yao, Y. R.; Jin, M.; Yang, W.; Zhang, X.; Li, X.; Zhang, D.; Zhao, Y.; Li, X.; Wang, S.; Echegoyen, L.; Autschbach, J.; Chen, N. Diuranium(IV) Carbide Cluster U₂C₂ Stabilized Inside Fullerene Cages. *J. Am. Chem. Soc.* **2019**, *141* (51), 20249–20260. <https://doi.org/10.1021/jacs.9b10247>.
- (23) Zhang, X.; Wang, Y.; Morales-Martínez, R.; Zhong, J.; de Graaf, C.; Rodríguez-Fortea, A.; Poblet, J. M.; Echegoyen, L.; Feng, L.; Chen, N. U₂@I_h(7)-C₈₀: Crystallographic Characterization of a Long-Sought Dimetallic Actinide Endohedral Fullerene. *J. Am. Chem. Soc.* **2018**, *140* (11), 3907–3915. <https://doi.org/10.1021/jacs.7b10865>.
- (24) Shen, Y.; Yu, X.; Meng, Q.; Yao, Y. R.; Autschbach, J.; Chen, N. ThC₂@C₈₂ versus Th@C₈₄: Unexpected Formation of Triangular Thorium Carbide Cluster inside Fullerenes. *Chem. Sci.* **2022**, *13* (44), 12980–12986. <https://doi.org/10.1039/d2sc04846a>.
- (25) Zhuang, J.; Morales-Martinez, R.; Zhang, J.; Wang, Y.; Yao, Y. R.; Pei, C.; Rodriguez-Fortea, A.; Wang, S.; Echegoyen, L.; de Graaf, C.; Poblet, J. M.; Chen, N. Characterization of a Strong Covalent Th³⁺–Th³⁺ Bond inside an I_h(7)-C₈₀ Fullerene Cage. *Nat. Commun.* **2021**, *12* (1), 2372. <https://doi.org/10.1038/s41467-021-22659-2>.